DRSAR-LEP-L

RIA-83-U311

AD

MEMORANDUM REPORT ARBRL-MR-03277

MULTIPHASE FLOW ANALYSIS OF THE BALLISTIC PERFORMANCE OF AN ANOMALOUS LOVA PROPELLANT MIX

Albert W. Horst

June 1983

US ARMY ARMAMENT RESEARCH AND DEVELOPMENT COMMAND
BALLISTIC RESEARCH LABORATORY
ABERDEEN PROVING GROUND, MARYLAND

UNCLASSIFIED

SECURITY CLASSIFICATION OF THIS PAGE *(When Data Entered)*

REPORT DOCUMENTATION PAGE

READ INSTRUCTIONS BEFORE COMPLETING FORM

1. REPORT NUMBER
MEMORANDUM REPORT ARBRL-MR-03277

2. GOVT ACCESSION NO.

3. RECIPIENT'S CATALOG NUMBER

4. TITLE *(and Subtitle)*
MULTIPHASE FLOW ANALYSIS OF THE BALLISTIC PERFORMANCE OF AN ANOMALOUS LOVA PROPELLANT MIX

5. TYPE OF REPORT & PERIOD COVERED
Memorandum Report
July-October 1982

6. PERFORMING ORG. REPORT NUMBER

7. AUTHOR(s)
Albert W. Horst

8. CONTRACT OR GRANT NUMBER(s)

9. PERFORMING ORGANIZATION NAME AND ADDRESS
US Army Ballistic Research Laboratory
ATTN: DRDAR-BLI
Aberdeen Proving Ground, MD 21005

10. PROGRAM ELEMENT, PROJECT, TASK AREA & WORK UNIT NUMBERS
1L161102AH43

11. CONTROLLING OFFICE NAME AND ADDRESS
US Army Armament Research and Development Command
US Army Ballistic Research Laboratory (DRDAR-BLA-S)
Aberdeen Proving Ground, MD 21005

12. REPORT DATE
June 1983

13. NUMBER OF PAGES
61

14. MONITORING AGENCY NAME & ADDRESS *(if different from Controlling Office)*

15. SECURITY CLASS. *(of this report)*
UNCLASSIFIED

15a. DECLASSIFICATION/DOWNGRADING SCHEDULE

16. DISTRIBUTION STATEMENT *(of this Report)*
Approved for public release; distribution unlimited

17. DISTRIBUTION STATEMENT *(of the abstract entered in Block 20, if different from Report)*

18. SUPPLEMENTARY NOTES

19. KEY WORDS *(Continue on reverse side if necessary and identify by block number)*

Interior Ballistics	Computer Codes
Guns	NOVA
Pressure Waves	Gun Propellants
Flamespread	LOVA

20. ABSTRACT *(Continue on reverse side if necessary and identify by block number)* mb

Low-vulnerability (LOVA) gun propellants offer an attractive approach to the reduction of the probability of catastrophic kill of armored weapon systems resulting from the initiation of on-board ammunition. The particular attributes of LOVA propellants which contribute to the desired impact on vulnerability include reduced ignitability and decreased burning rates at low pressures. These same characteristics, however, may influence other aspects of the ballistic cycle, unintended and unexpected by the propellant/charge

DD FORM 1 JAN 73 1473 EDITION OF 1 NOV 65 IS OBSOLETE

UNCLASSIFIED

SECURITY CLASSIFICATION OF THIS PAGE *(When Data Entered)* designer. In this paper, the interplay of these various features is investigated, specifically in respect to the anomalous ballistic performance of a particular LOVA propellant mix, by means of a two-phase flow interior ballistic code (NOVA), and the potential impact on gun performance is discussed.

TABLE OF CONTENTS

LIST OF ILLUSTRATIONS

LIST OF TABLES

I. INTRODUCTION

For several years now the US Army and Navy have been working jointly on a program to develop low vulnerability (LOVA) gun propellants. This effort was undertaken in response to the need to reduce the catastrophic kill of armored weapons systems by damage-inflicted initiation of on-board ammunition. The result has been development of a family of LOVA propellants, generally consisting of a nitramine (RDX or HMX) dispersed in an inert binder matrix. These formulations are characterized by an impetus level of 970 to 1100 J/g, with flame temperatures from 2280 to 2800 K. Ignition temperatures, according to conductive ignition tests, are in the range of 600 to 1300 K, and burning rate exponents are typically reported to be just in excess of unity. Documentation abounds on the LOVA program, and the reader is directed to the references for a more complete discussion of this major research and development effort and its accomplishments.[1,2]

The reduction in vulnerability offered by LOVA propellants can, in general, be associated with two characteristics of these formulations. Primarily, a higher threshold for thermal ignition reduces the likelihood of inadvertent initiation, or at least delays its onset and reduces the rate of subsequent flamespread. In addition, lower burning rates at low pressures reduce local pressurization rates, again likely slowing flamespread, perhaps even eliminating conditions which might otherwise contribute to the transfer of ignition among stored ammunition components.

Some of these same features, however, may have impact on various aspects of the interior ballistic cycle beyond that of ignition. For instance, the reduction in burning rates at low pressures is most often accompanied by some increase in the sensitivity of burning rate to pressure, manifested in a burning rate pressure exponent in excess of unity. Classical ballistic considerations suggest that this should result in a small overall increase in ballistic variability,[3] an effect which indeed has been noted during some LOVA gun firings. Further, it has been noted that, while development efforts to date have been directed towards tank guns, low-pressure ignition and combustion characteristics exhibited by LOVA propellants may pose considerable

---

[1] *S. Wise and J.J. Rocchio, "Binder Requirements for Low Vulnerability Propellants," 18th JANNAF Combustion Meeting, CPIA Publication 347, Vol. II, pp. 305-320, October 1981.*

[2] *R.W. Deas, G.E. Keller, and J.J. Rocchio, "The Interior Ballistic Performance of Low Vulnerability Ammunition (LOVA)," 1981 JANNAF Propulsion Meeting, CPIA Publication 340, Vol. III, pp. 437-477, May 1981.*

[3] *A.C. Haukland and W.M. Burnett, "Sensitivity of Interior Ballistic Performance to Propellant Thermochemical Parameters," Proceedings of the Tri-Service Gun Propellant Symposium, Vol. I, pp. 7.3-1 - 7.3-11, Picatinny Arsenal, Dover, NJ, October 1972.*

difficulties to the designer of zoned, artillery charges.[4] In this study, however, we will limit ourselves to the influence of these features on multiphase flow processes, including ignition and flamespread, in the tank gun configuration currently of interest.

II. DISCUSSION

A. Background

Let us begin with a brief review of multiphase flow processes typically occurring in conventional, high-performance propelling charges employing granular propellant. The sequence of events begins with a local ignition stimulus of hot gases and/or particles, which for tank ammunition employing a high-pressure bayonet primer, results in ignition of adjacent propellant grains in just a few milliseconds. Combustion products from the burning grains join those from the igniter, penetrating the remainder of the propellant bed and leading to convectively driven flame propagation throughout the entire propellant charge. Concurrently, interphase drag may lead to local bed compaction, which is similarly transmitted through the propellant aggregate, and motion, with possible impact of individual grains against the projectile base or breech face. Stagnation and reflection of the gas pressure wave associated with the ignition front at these same boundaries increase local pressures and hence local propellant burning rates. This situation may be further exacerbated by a reduction in local free volume if bed compaction is present or by additional burning surface if grain fracture has occurred.

Tank ammunition has often been considered relatively immune to the vigorous multiphase flow dynamics described above because of the nearly uniform, distributed igniter output provided by bayonet primers and immobility of the propellant bed in a nearly full cartridge case. Recent years, however, have seen more and more tank ammunition configurations with long projectile boattails extending deep into the propellant bed, preventing use of the traditional long, bayonet primer. Moreover, the tapered portion of the boattail provides a region of changing cross-sectional area which could serve to focus gas pressure waves and perhaps easily distort incoming propellant grains to the point of fracture.

The study reported herein was motivated by the results from a series of firings in a 105-mm, M68 Tank Gun performed to evaluate the ballistic performance of a particular LOVA formulation (CAB/ATEC/RDX, Mix 1453). Substantial variations in maximum chamber pressure were observed; further, maximum chamber pressure was seen to increase with increasing levels of pressure waves, as measured in terms of the initial reverse pressure difference between breech and forward ends of the gun chamber. (See Figure 1 and Appendix A.) This relationship between pressure waves and maximum chamber pressure is well

---

[4] *T.C. Minor and A.W. Horst, "Some Experimental Methods for the Study of Two-Phase Flow in LOVA Artillery Charges,"* <u>*Internationale Jahrestagung*</u>*, ICT, Karlsruhe, Germany, June 1982.*

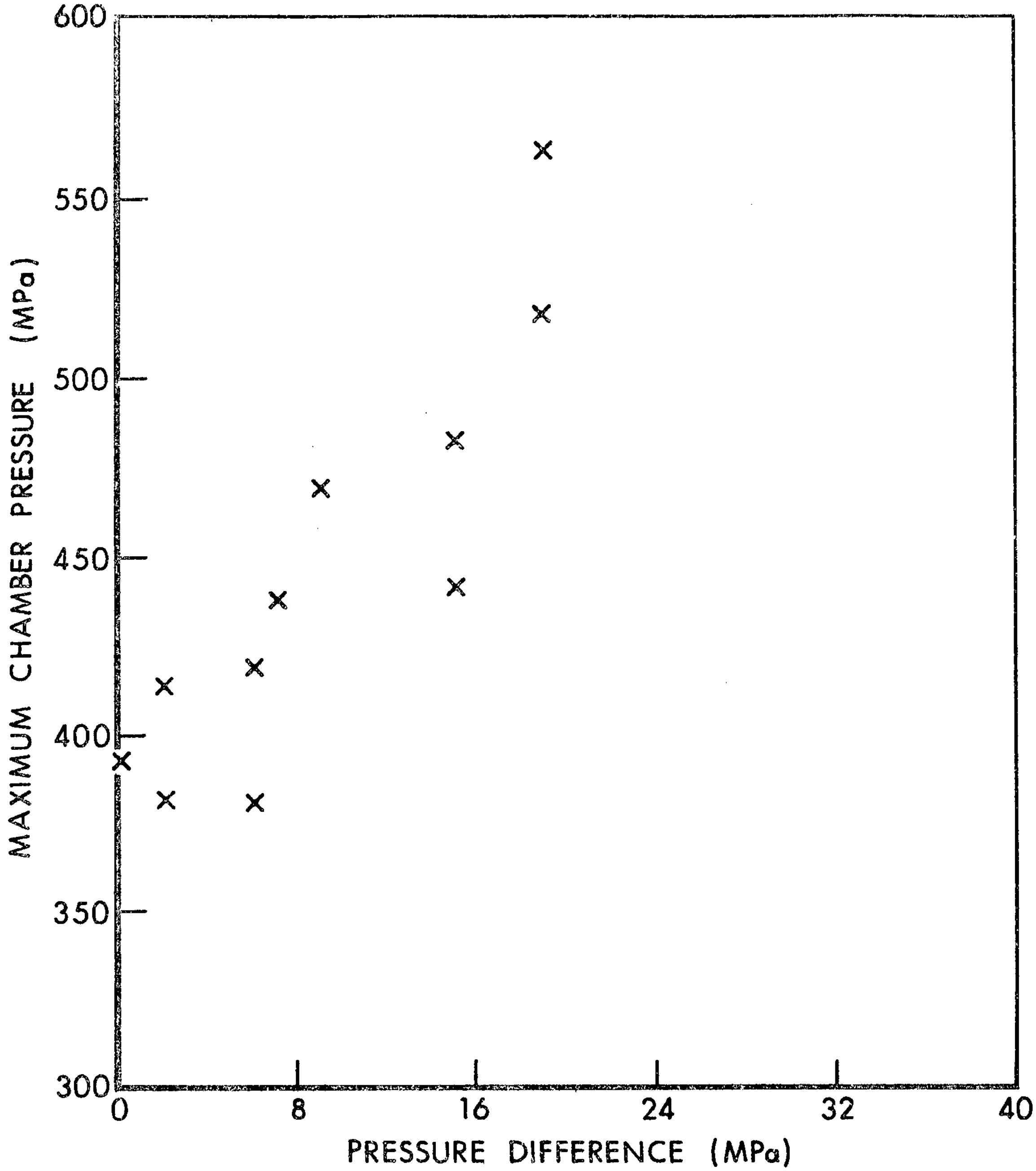

Figure 1. Maximum Chamber Pressure Versus Initial Reverse Pressure Difference, Experimental

documented for artillery charges,[5] where variations in igniter stimulus and propellant/chamber interface are readily available to excite strong, longitudinal pressure waves leading to grain fracture, but a similar exhibition by tank ammunition, supposedly free from such variables, requires that comparable yet unknown mechanisms be operative. This work was thus undertaken to identify any such mechanisms and to ensure their absence in developmental propelling charges employing candidate LOVA propellants.

B. Analysis

The analysis was performed using the NOVA code,[6] a two-phase, unsteady flow representation of the interior ballistic cycle. The balance equations describe the evolution of macroscopic flow properties accompanying changes in mass, momentum, and energy arising out of interactions associated with combustion, interphase drag, and heat transfer. Functioning of the igniter is included by specifying a predetermined mass injection rate as a function of position and time. Flamespread then follows from axial convection, with grain surface temperature deduced from a heat transfer correlation and the unsteady heat conduction equation, and ignition based on a surface temperature criterion. The NOVA code provides a one-dimensional (with area change) representation of flow, necessitating some compromise in configural aspects of the problem, as depicted in Figure 2. It was felt, however, that this limitation would not seriously degrade the essential feature of the study - assessing the ballistic influence of propellant characteristics unique to the LOVA family. If results warranted further attention to the problem, a somewhat more costly two-dimensional analysis could be performed using the TDNOVA code.[7]

A baseline NOVA calculation for the 105-mm, M68 Tank Gun firing the M456 Cartridge loaded with 5.76 kg of LOVA propellant (CAB/ATEC/RDX, Mix 1453) was performed using input data displayed in Table 1. A predicted maximum chamber pressure of about 450 MPa, obtained with no attempt to manipulate barrel resistance or burning rate data for refinement of the calculation, falls comfortably in the range of values shown in Figure 1. Further, the predicted structure of pressure versus time and pressure-difference versus time profiles is in surprisingly good agreement with experimental data recorded for one of the rounds exhibiting a relatively low level of pressure waves. (See Figure 3.)

Calculations were then performed to determine the role played in characterization of the ballistic environment by those particular inputs exhibiting

---

[5] *A.W. Horst, I.W. May, and E.V. Clarke, "The Missing Link Between Pressure Waves and Breechblows," ARBRL-MR-02849, USA ARRADCOM, Ballistic Research Laboratory, Aberdeen Proving Ground, MD, July 1978 (AD A058354).*

[6] *P.S. Gough, "The NOVA Code: A User's Manual. Volume 1. Description and Use," IHCR 80-8, Naval Ordnance Station, Indian Head, MD, December 1980.*

[7] *P.S. Gough, "A Two-Dimensional Model of the Interior Ballistics of Bagged Artillery Charges," ARBRL-CR-00452, USA ARRADCOM, Ballistic Research Laboratory, Aberdeen Proving Ground, MD, April 1981 (AD A100751).*

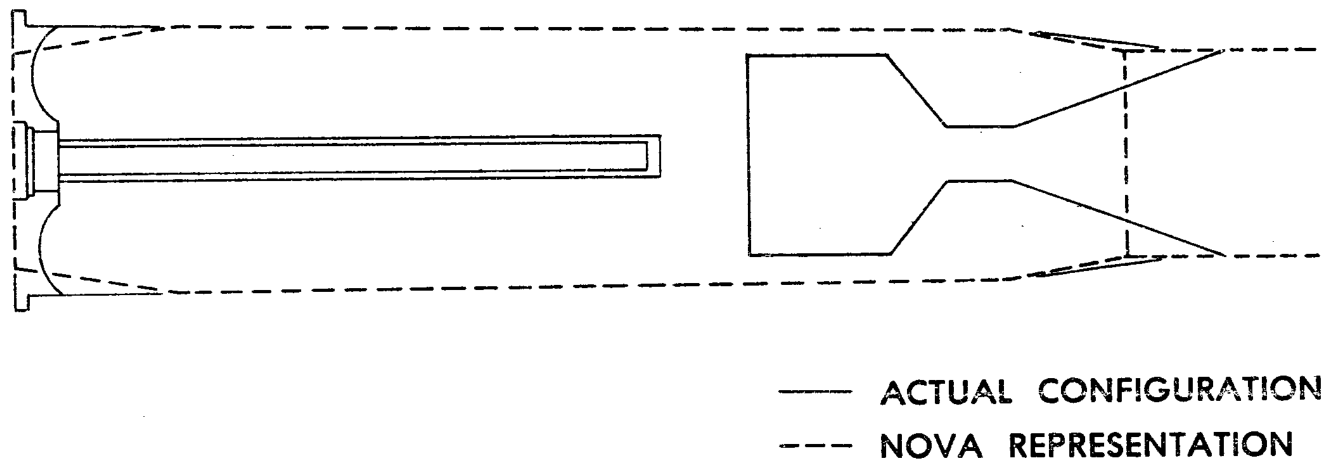

Figure 2. Actual Ammunition/Tube Interface and NOVA Code Representation

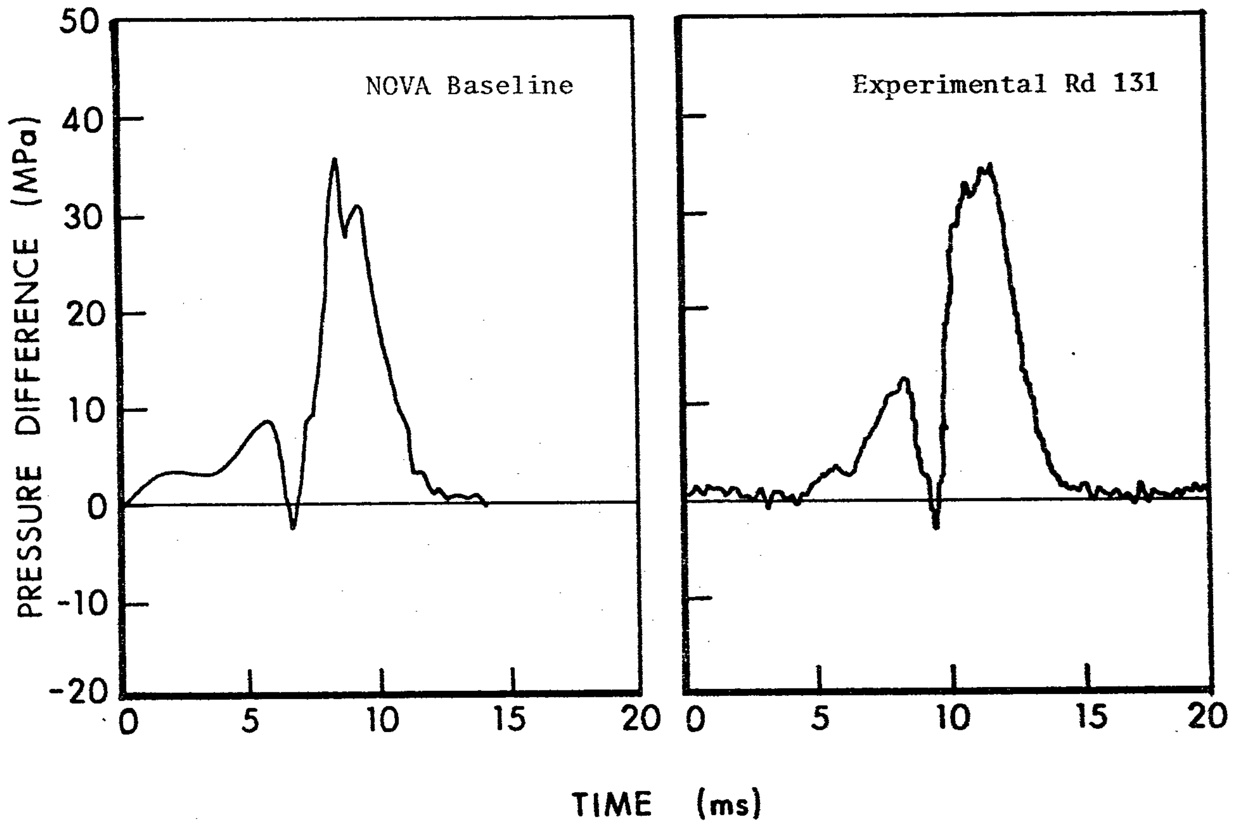

Figure 3. Comparison of Calculated and Experimental Pressure-Difference Profiles

TABLE 1. PROPELLANT INPUT DATA

PROPELLANT TYPE	CAB/ATEC/RDX
MASS OF PROPELLANT (kg)	5.76
DENSITY OF PROPELLANT (g/cm^3)	1.58
OUTSIDE DIAMETER (mm)	4.39
PERFORATION DIAMETER (mm)	0.28
LENGTH (mm)	6.50
NUMBER OF PERFORATIONS	7
SPEED OF COMPRESSION WAVE IN SETTLED BED (m/s)	152.
SPEED OF EXPANSION WAVE (m/s)	1270.
BURNING RATE COEFFICIENT ($cm/s \cdot MPa^{EXP}$)	0.02573
BURNING RATE EXPONENT	1.05
BURNING RATE ADDITIVE CONSTANT	0.
IGNITION TEMPERATURE (K)	611.
THERMAL CONDUCTIVITY ($J/cm \cdot s \cdot K$)	0.00222
THERMAL DIFFUSIVITY (cm^2/s)	0.0008677
EMISSIVITY FACTOR	0.6
CHEMICAL ENERGY RELEASED IN BURNING (J/g)	3716.
MOLECULAR WEIGHT (g/gmol)	20.22
RATIO OF SPECIFIC HEATS	1.275
COVOLUME (cm^3/g)	1.19

values largely unique to LOVA propellants. Specifically addressed were burning rates and ignition temperatures, for reasons previously discussed, and propellant rheology, largely uncharacterized for this family of propellants. In addition, the influence of igniter profiles reflecting increasing levels of local base ignition was studied, as was the sensitivity of results to projectile engraving pressure.

Of immediate notice is the substantial variation in predicted performance observed to accompany selected modifications to the input data base. Treating the less intriguing results first, we note in Table 2 a relatively small and qualitatively reasonable influence of propellant bed rheology as reflected in the speed of compression waves in the settled bed. The slightly stiffer bed of the modified data base led to less bed compaction at stagnation and a slight reduction in the level of predicted pressure waves. However, the influence of engraving pressure on maximum chamber pressure and muzzle velocity was quite large, though there was surprisingly little impact on predicted pressure-wave level. Indeed, a somewhat more conscientious study of the pressure-difference versus time profiles revealed very similar pressure waves superimposed with little coupling on quite disparate overall chamber-pressure levels associated with differences in projectile motion. (A complete set of all pressure-difference profiles calculated using the NOVA code during the course of this study is included as Appendix B.)

A totally unexpected result was the strong influence of ignition temperature on calculated results shown in Table 3. Realizing that the use of a surface-temperature ignition criterion represents quite a simplification of nature, particularly in the highly transient gun environment, we wish to de-

TABLE 2. SUMMARY OF CALCULATED RESULTS - BASELINE

STUDY PARAMETER	MAX PRESS (MPa)	MUZ VELOCITY (m/s)	DIFF PRESS (MPa)
Baseline (Table 1)	447	1211	3
Speed of Compression Wave = 254 m/s	441	1207	0
Engraving Pressure = 21 MPa (34 MPa baseline)	372	1154	3
Engraving Pressure = 48 MPa	498	1241	1

emphasize the importance of the actual input values employed in the study. Nevertheless, the fact that the range of ignition temperatures studied exerted an influence on predicted pressures, velocities, and pressure waves alike suggests that this aspect of LOVA propellants may be playing a role of ballistic consequence beyond the intended reduction in vulnerability. Again, the important parameters here seem to be just how much propellant is burning at what pressures and associated burning rates before the projectile experiences significant travel.

TABLE 3. SUMMARY OF CALCULATED RESULTS - IGNITION TEMPERATURE

STUDY PARAMETER	MAX PRESS (MPa)	MUZ VELOCITY (m/s)	DIFF PRESS (MPa)
Baseline (Table 1)	447	1211	3
Ignition Temp = 444 K	372	1159	18
Ignition Temp = 528 K	386	1170	12
Ignition Temp = 694 K	--- propellant did not ignite ---		

Remaining for the moment with the topic of ignition, we note in Table 4 that increased levels of localized, base ignition of the propellant charge are predicted, as expected, to lead to an increase in the magnitude of pressure

TABLE 4. SUMMARY OF CALCULATED RESULTS - IGNITER PROFILE

STUDY PARAMETER	MAX PRESS (MPa)	MUZ VELOCITY (m/s)	DIFF PRESS (MPa)
Baseline (Table 1)	447	1211	3
Base/Forward Igniter Output Ratio = 2 (Baseline = 1)	419	1189	8
Base/Forward Igniter Output Ratio = 3	372	1150	9

waves. However, unlike the experimental data of Figure 1, a reduction, rather than an increase, in maximum chamber pressure is seen to accompany this trend. We will return to this disconcerting result shortly.

An earlier study [8] documented the predicted influence of burning rate representation on predicted pressure waves in a Navy 5-Inch/54-Caliber Gun. When the burning rate exponent is reduced and the coefficient correspondingly increased to maintain overall ballistic levels in a particular gun environment, low pressure burning rates are seen to increase, most often increasing pressure-wave levels as well. On the other hand, as seen in the results of the current study (Table 5), increasing the exponent and decreasing the coefficient in a similar fashion may so reduce low pressure burning rates that the flame does not propagate if only a small portion of the propellant bed is ignited directly by the primer. Additional results were obtained here by simultaneously reducing the ignition temperature to increase the size of this region ignited by the primer. The strong link between burning rate and pressure waves previously documented was then reproduced, though we must note that the accompanying trend in maximum chamber pressure is unfortunately more a result of our scheme for selecting burning rate coefficients than an expression of the correct physical relationship between maximum pressure and pressure waves.

TABLE 5. SUMMARY OF CALCULATED RESULTS - BURNING RATE EXPONENT

STUDY PARAMETER	MAX PRESS (MPa)	MUZ VELOCITY (m/s)	DIFF PRESS (MPa)
Baseline (Table 1)	447	1211	3
Burning Rate Exponent = 1.0	442	1203	9
Burning Rate Exponent = 1.1	441	calculation not completed	--
Burning Rate Exponent = 1.2	----	flame did not propagate	---
Burning Rate Exponent = 1.0; Ignition Temp = 444 K	383	1167	23
Burning Rate Exponent = 1.1; Ignition Temp = 444 K	359	1148	14
Burning Rate Exponent = 1.2; Ignition Temp = 444 K	339	1126	9

[8] *A.W. Horst, "Influence of Burning Rate Representation on Gun Environment Flamespread and Pressure Wave Predictions," IHMR 76-255, Naval Ordnance Station, Indian Head, MD, March 1976.*

We also note that while burning rates were originally provided to this investigator in terms of a single set of values for b and n in the classical $r=bP^n$ representation, actual closed bomb data, shown in Figure 4, reveal the presence of several apparent slope breaks. While two of these inflections occur at low pressures and are possibly complicated by flamespreading phenomena, the slope break near 100 MPa cannot be so easily discredited. The actual burning rate exponent in the highest pressure region shown ranges from 1.17 to 1.32, depending on treatment of the trailoff at the top end of the data. The results of several calculations using these data (Table 6) attest to the fact that ballistic performance is extremely sensitive to burning rates and that, at these high exponents, overall system ballistic sensitivity to other perturbations (e.g., variations in projectile weight, charge weight, or, as demonstrated here, engraving pressure) may be substantially increased. In the calculations reported, a change in peak engraving pressure from 21 to 34 MPa yielded increases in maximum chamber pressure of 75 and 201 MPa for the runs employing burning rate exponents of 1.05 and 1.17 respectively!

TABLE 6. SUMMARY OF CALCULATED RESULTS - MULTI-SLOPE BURNING RATES

STUDY PARAMETER	MAX PRESS (MPa)	MUZ VELOCITY (m/s)	DIFF PRESS (MPa)
Baseline (Table 1)	447	1211	3
Multi-Slope; High-Pressure Exponent = 1.32	1234	1393	11
Multi-Slope; High-Pressure Exponent = 1.17	561	1280	11
Multi-Slope; High-Pressure Exponent = 1.17; Engraving Pressure = 21 MPa	360	1158	6
Multi-Slope; High-Pressure Exponent = 1.17; Engraving Pressure = 28 MPa	458	1232	10

A relevant selection of results from the above calculations is depicted graphically in Figure 5, where predictions of maximum chamber pressure and the corresponding pressure-wave level are displayed. The predicted trend, if any, is not very satisfying in light of experimental results. Clearly, some process is occurring in the 105-mm gun that is not being captured in the NOVA simulations. This result, however, is not unprecedented, and indeed has been discussed in some detail in a previously referenced publication,[5] where the missing link was postulated to be grain fracture. If we explore our calculations in somewhat more detail, we note that increasing levels of bed compac-

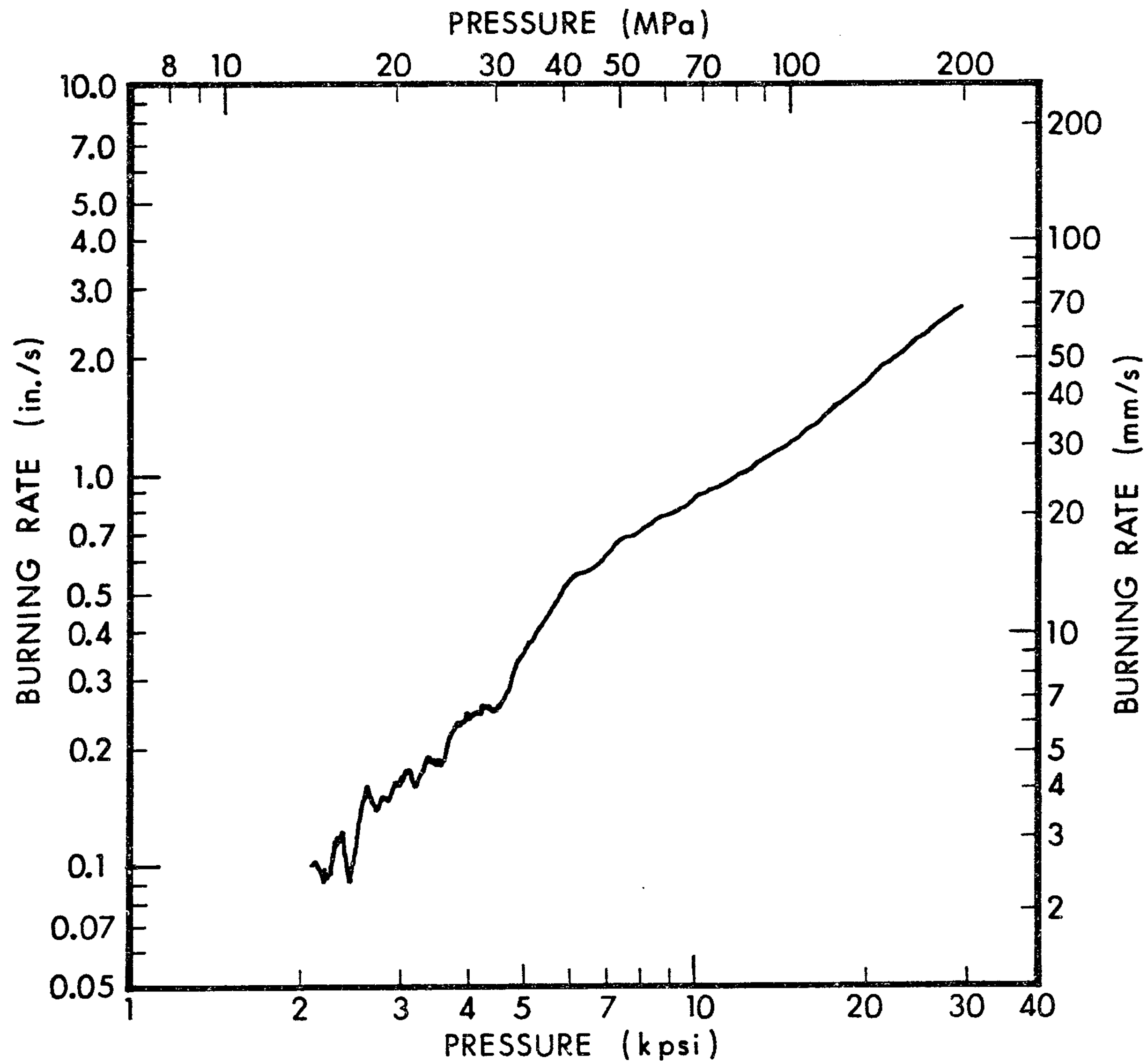

Figure 4. Closed Bomb Burning Rate Data for Test Propellant

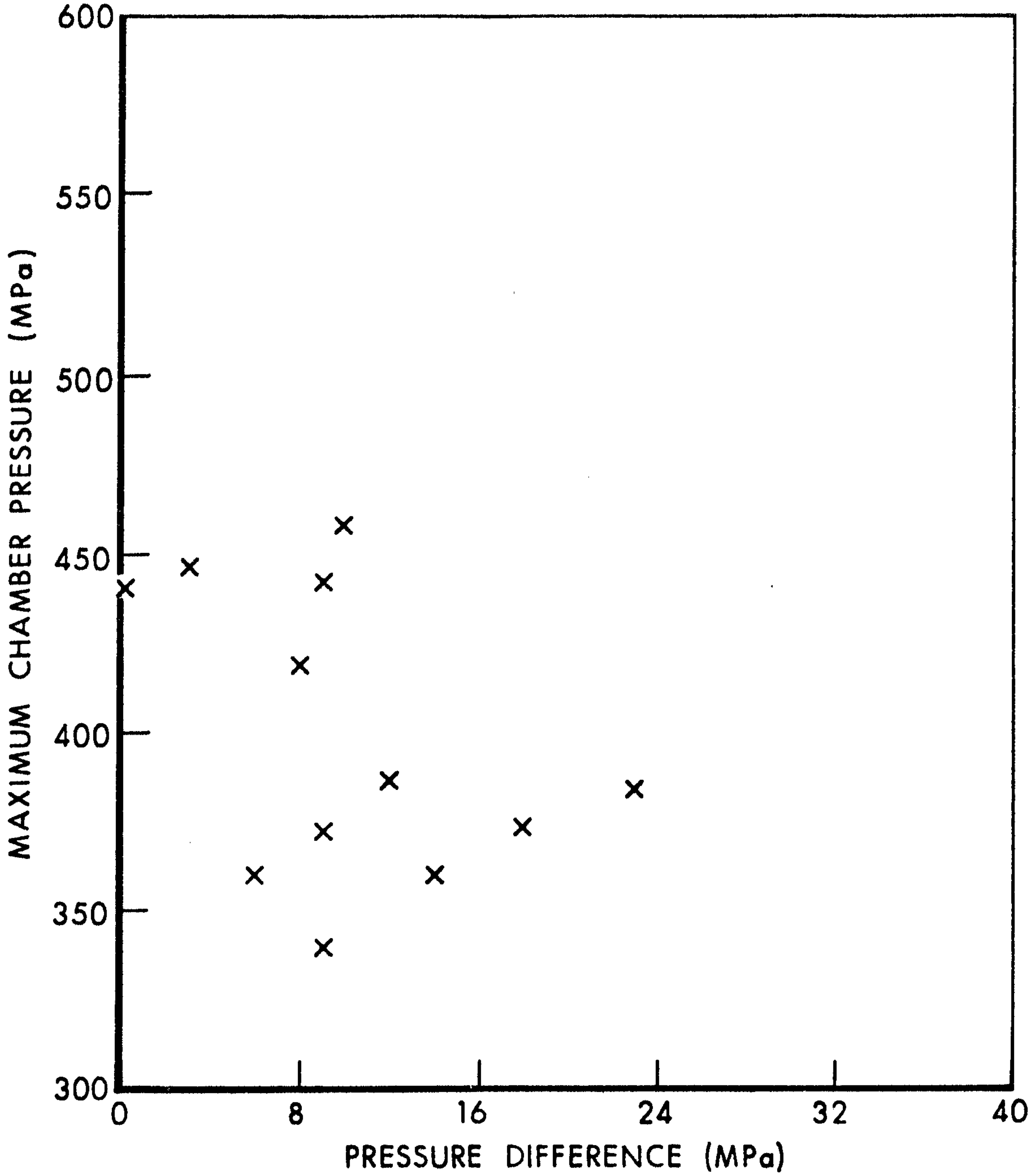

Figure 5. Maximum Chamber Pressure Versus Initial Reverse Pressure Difference, Calculated

tion and accompanying intergranular stress at the forward edge of the propellant bed are associated with increases in the magnitude of predicted pressure waves. These relationships have been included as Figures 6 and 7 and, if realistic, are very likely to result in grain fracture in the gun -- even if not in the NOVA code!

In response to this possibility, several special NOVA calculations were performed to determine the influence of localized grain fracture in this region of high intergranular stress. To simulate this process, the calculation was halted at the appropriate time and the forward 10 cm of propellant were "fractured," as indicated in Figure 8, yielding local increases in surface area of about 3 1/2 and 6 times that of the unaltered grains. (We note that the cylindrical "splinters" shown are not necessarily believed to reflect the actual configuration of shattered grains but are simply employed to facilitate numerical treatment of the problem.) The calculation was then resumed with this increased burning surface locally concentrated in the front of the gun chamber. Ignition temperatures were also manipulated between 444 and 694 K to allow investigation of this event both when the newly fractured grains had previously been ignited and when flamespread had not quite reached this portion of the charge. The data shown in Table 7 reflect the results from this series of NOVA runs, both identifying a mechanism capable of substantial impact on maximum chamber pressures and confirming the earlier result that variations in flamespreading properties could be one source of ballistic irreproducibility with LOVA propellants.

TABLE 7. SUMMARY OF CALCULATED RESULTS - GRAIN FRACTURE

STUDY PARAMETER	MAX PRESS (MPa)	MUZ VELOCITY (m/s)	DIFF PRESS (MPa)
Baseline (Table 1)	447	1211	3
Baseline with Ignition Temperature = 444 K	372	1159	18
Fracture Diameter = 1.8 mm; Ignition Temperature = 694 K	397	1178	20
Fracture Diameter = 1.8 mm; Ignition Temperature = 444 K	397	1180	23
Fracture Diameter = 0.9 mm; Ignition Temperature = 694 K	483	calculation not completed	19
Fracture Diameter = 0.9 mm; Ignition Temperature = 444 K	534	1259	41

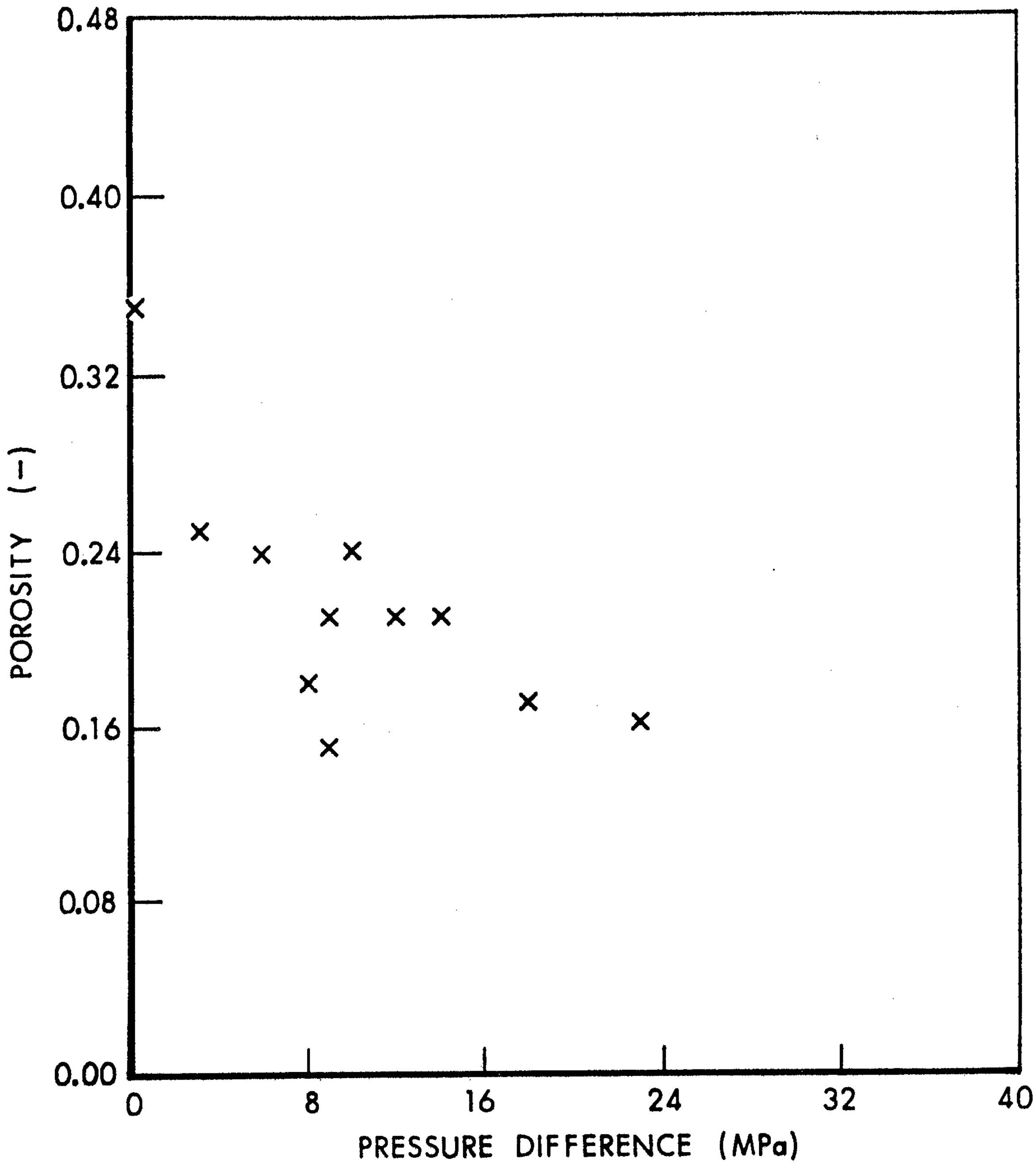

Figure 6. Minimum Bed Porosity Versus Initial Reverse Pressure Difference, Calculated

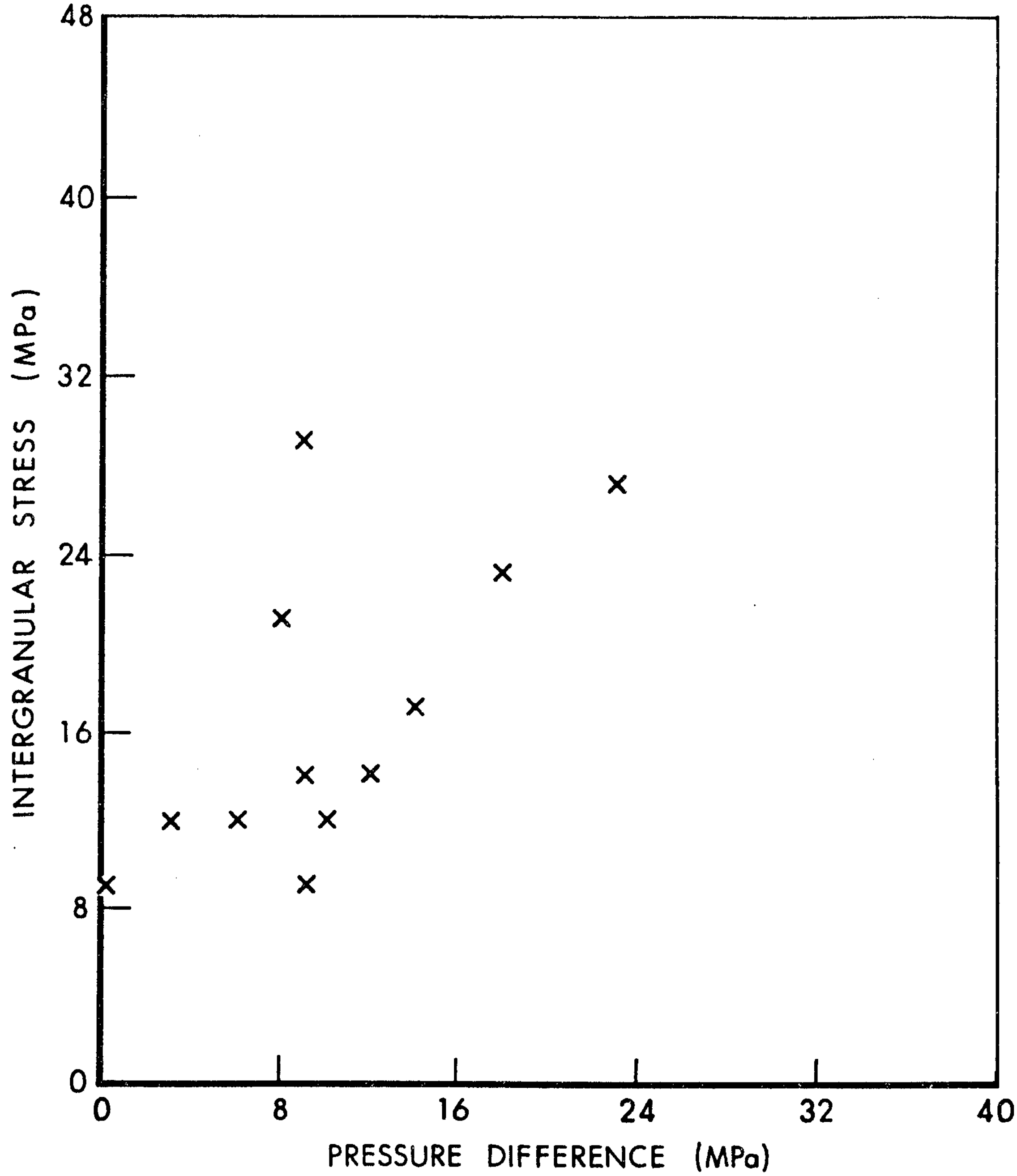

Figure 7. Maximum Intergranular Stress Versus Initial Reverse Pressure Difference, Calculated

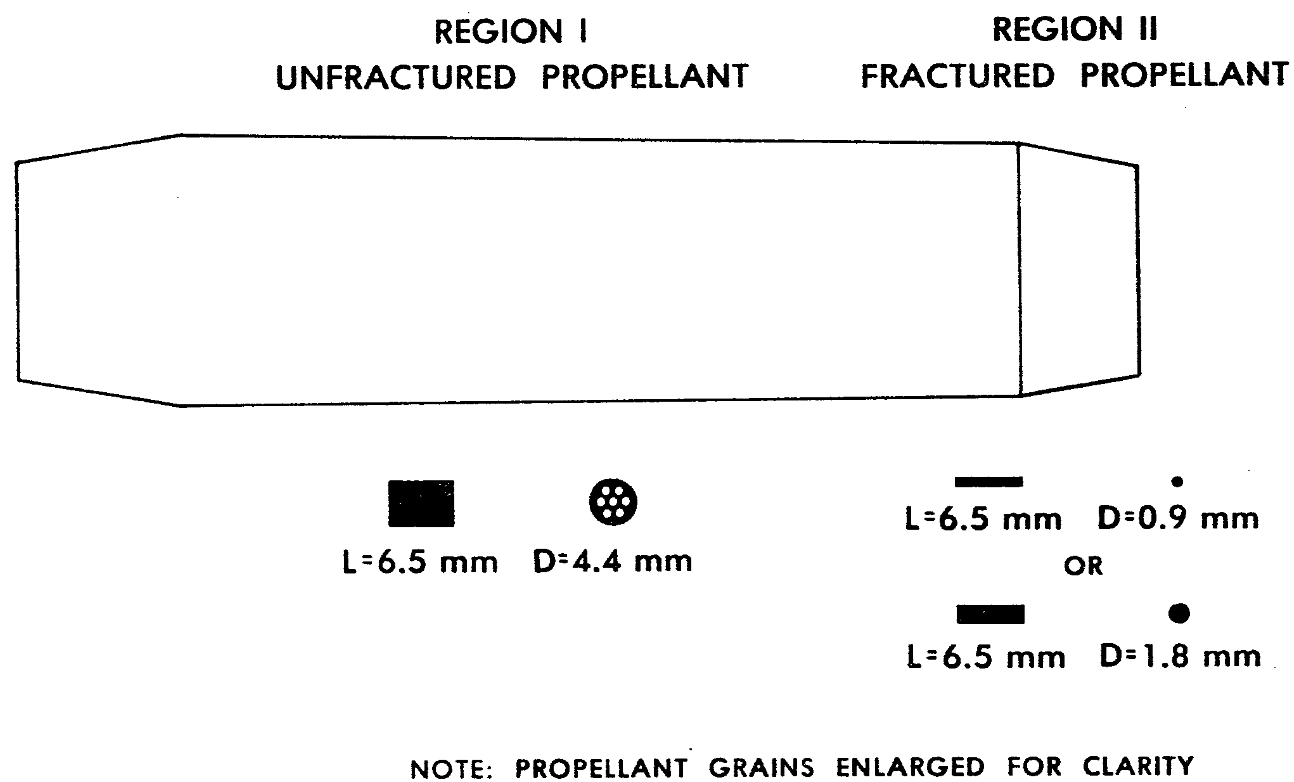

Figure 8. NOVA Code Representation of Grain "Fracture"

III. CONCLUSIONS

While the above analysis involved many simplifications of both physical and chemical aspects of the propellant system under study, the following conclusions can be drawn from calculated results:

1. Performance variability experienced during ballistic testing of LOVA propellant Mix 1453 and very likely for any other propellant exhibiting similar combustion properties may be, in some significant part, a result of variations in the extent of flamespread at first motion of the projectile. This result underscores the need for reproducibility of both propellant ignitability and primer performance.

2. Performance variability for such propellants will also be exacerbated by an increased system sensitivity associated with high burning rate exponents. Burning rate data over the entire range encountered in the gun are necessary to assure propellant acceptability and reproducibility; a single bP^n description fit over the entire range will most often not be useful to this end and perhaps may even be misleading.

3. Neither of the above mechanisms, however, is sufficient to explain the apparent relationship between maximum chamber pressure and pressure waves. While they may be responsible for a variation in the magnitude of the pressure waves themselves, propellant grain fracture, caused by the accompanying high levels of intergranular stress, is once again implicated as the likely link between increases in pressure waves and increases in maximum chamber pressure.

REFERENCES

1. S. Wise and J.J. Rocchio, "Binder Requirements for Low Vulnerability Propellants," 18th JANNAF Combustion Meeting, CPIA Publication 347, Vol. II, pp. 305-320, October 1981.

2. R.W. Deas, G.E. Keller, and J.J. Rocchio, "The Interior Ballistic Performance of Low Vulnerability Ammunition (LOVA)," 1981 JANNAF Propulsion Meeting, CPIA Publication 340, Vol. III, pp. 437-477, May 1981.

3. A.C. Haukland and W.M. Burnett, "Sensitivity of Interior Ballistic Performance to Propellant Thermochemical Parameters," Proceedings of the Tri-Service Gun Propellant Symposium, Vol. I, pp. 7.3-1 - 7.3-11, Picatinny Arsenal, Dover, NJ, October 1972.

4. T.C. Minor and A.W. Horst, "Some Experimental Methods for the Study of Two-Phase Flow in LOVA Artillery Charges," Internationale Jahrestagung, ICT, Karlsruhe, Germany, June 1982.

5. A.W. Horst, I.W. May, and E.V. Clarke, "The Missing Link Between Pressure Waves and Breechblows," ARBRL-MR-02849, USA ARRADCOM, Ballistic Research Laboratory, Aberdeen Proving Ground, MD, July 1978 (AD A058354).

6. P.S. Gough, "The NOVA Code: A User's Manual. Volume 1. Description and Use," IHCR 80-8, Naval Ordnance Station, Indian Head, MD, December 1980.

7. P.S. Gough, "A Two-Dimensional Model of the Interior Ballistics of Bagged Artillery Charges," ARBRL-CR-00452, USA ARRADCOM, Ballistic Research Laboratory, Aberdeen Proving Ground, MD, April 1981 (AD A100751).

8. A.W. Horst, "Influence of Burning Rate Representation on Gun Environment Flamespread and Pressure Wave Predictions," IHMR 76-255, Naval Ordnance Station, Indian Head, MD, March 1976.

APPENDIX A

EXPERIMENTAL PRESSURE VERSUS TIME AND PRESSURE DIFFERENCE VERSUS TIME PROFILES

LOVA-IHEP: CAB/ATEC SERIES ROUND: 130

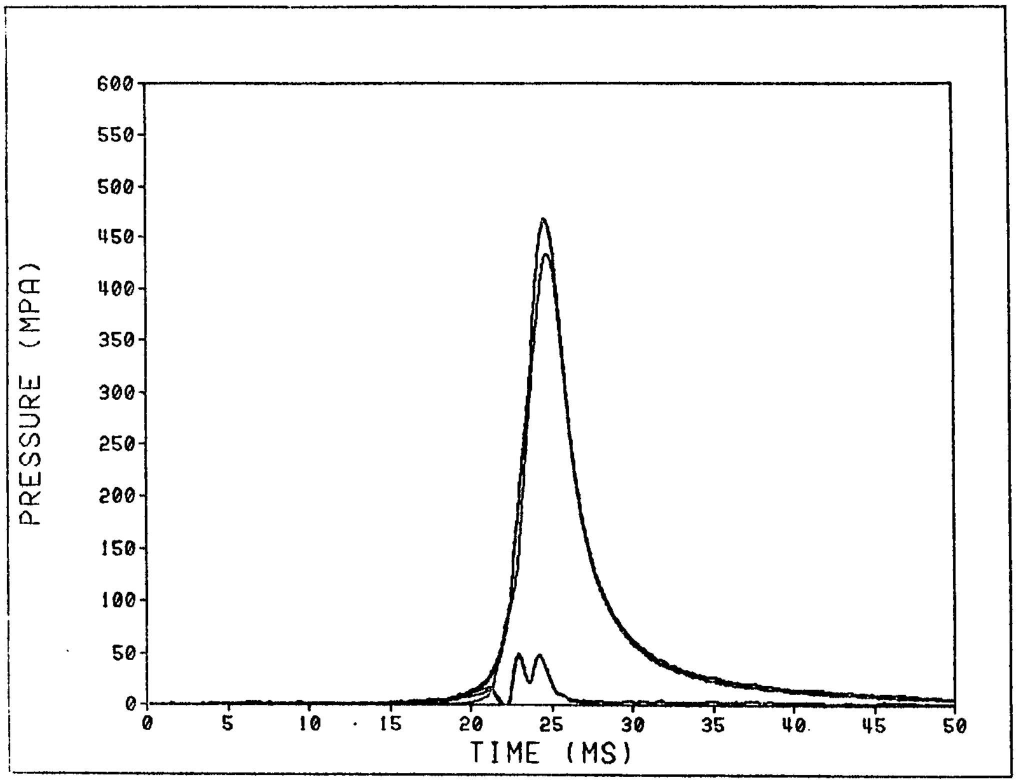

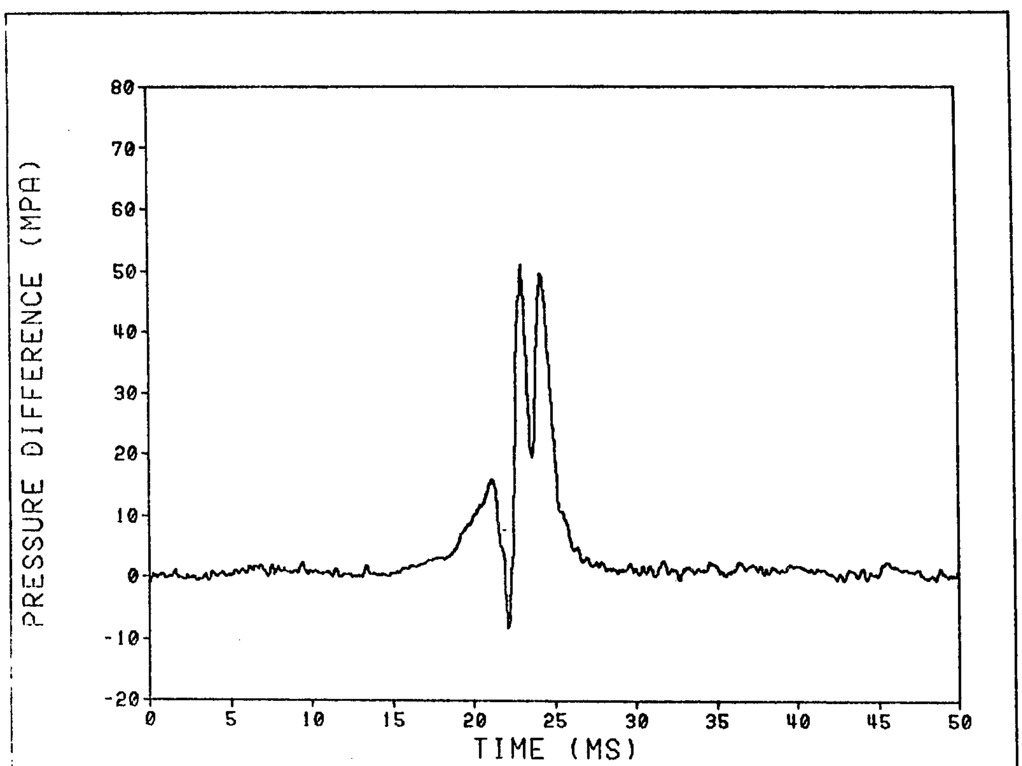

LOVA-IHEP: CAB/ATEC SERIES ROUND: 131

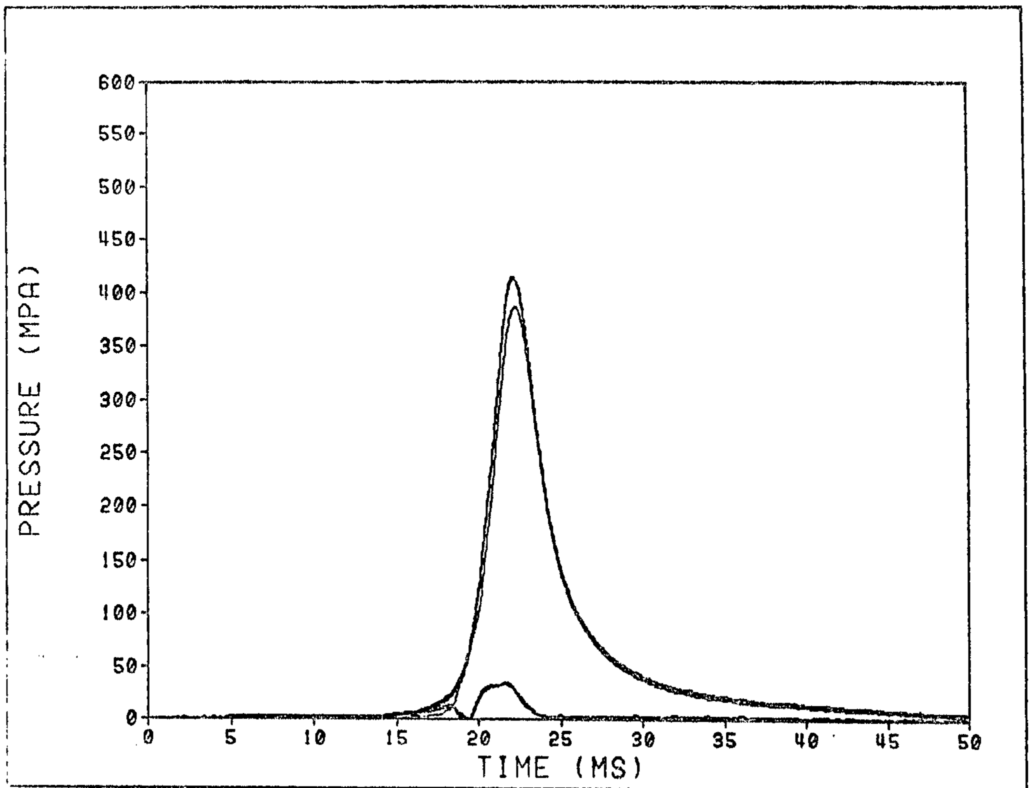

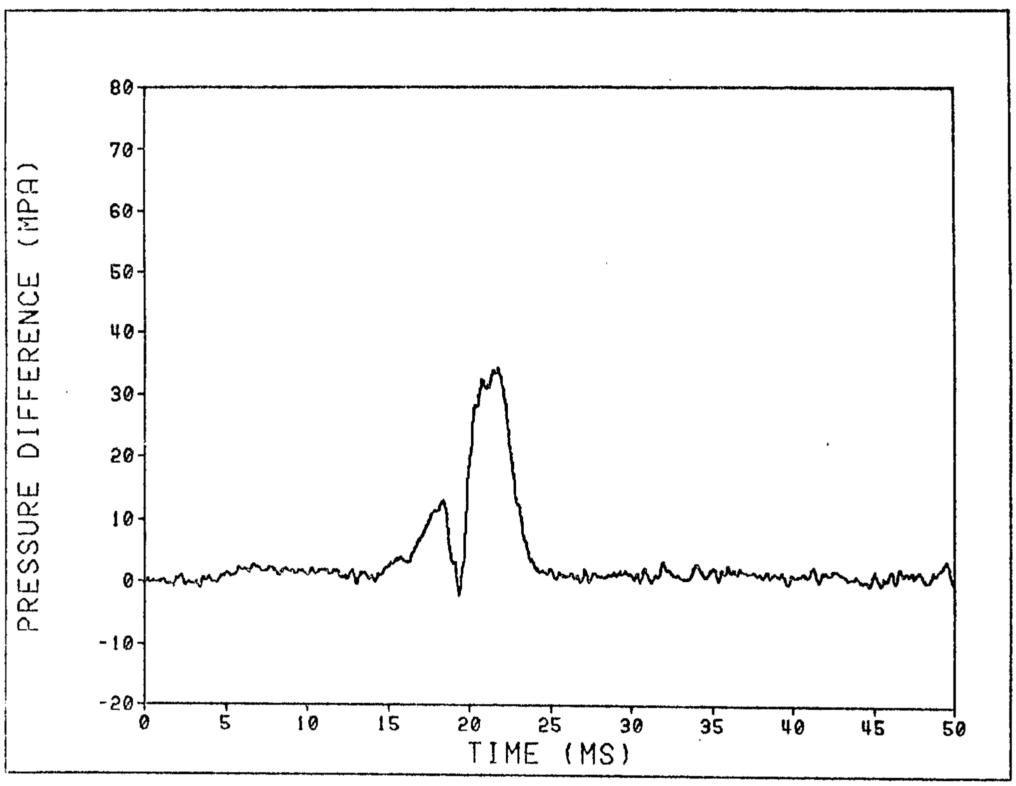

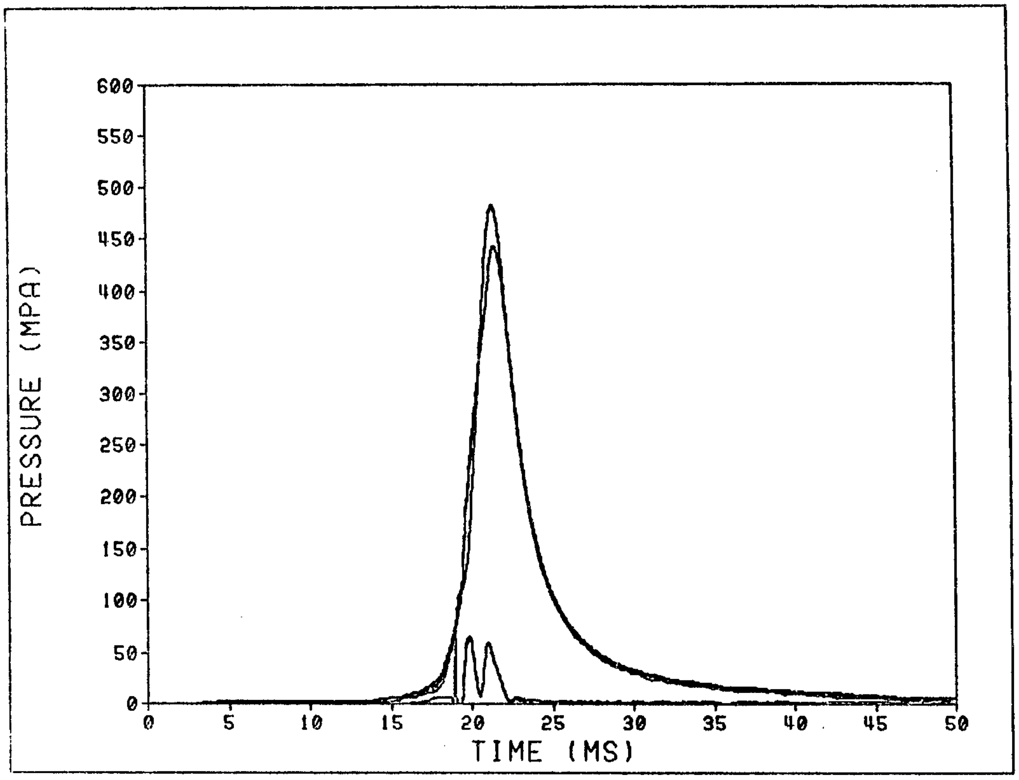
PRESSURE (MPA)
600
550
500
450
400
350
300
250
200
150
100
50
0
0
5
10
15
20
25
30
35
40
45
50
TIME (MS)

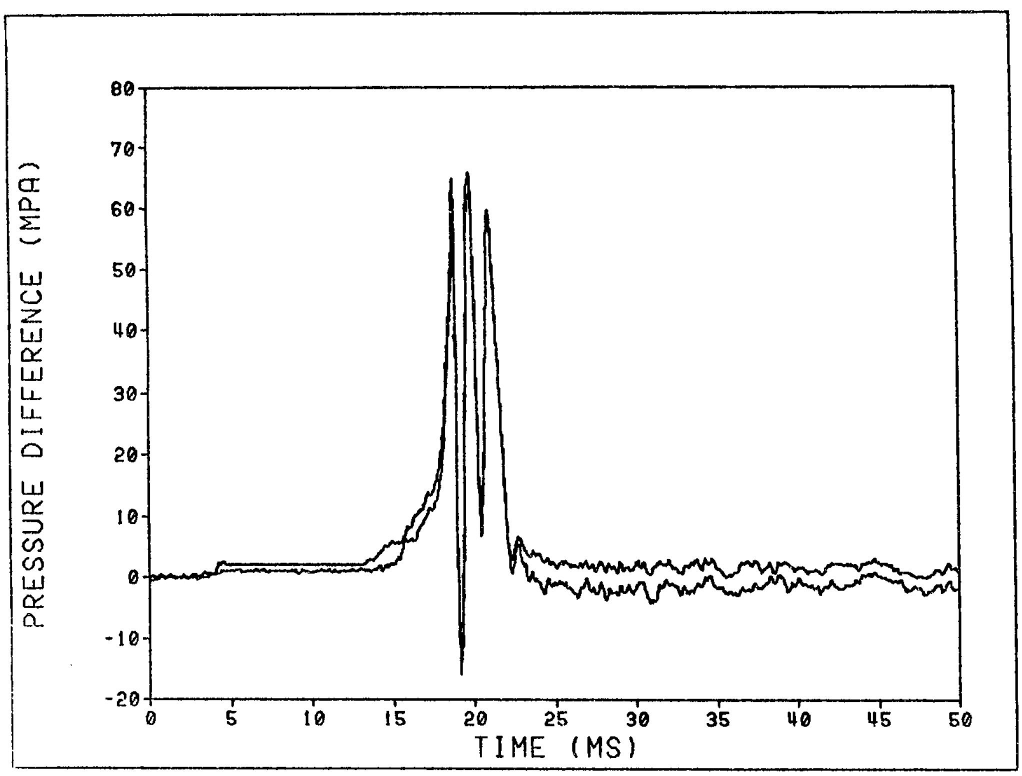
PRESSURE DIFFERENCE (MPA)
80
70
60
50
40
30
20
10
0
-10
-20
0
5
10
15
20
25
30
35
40
45
50
TIME (MS)

LOVA-IHEP: CAB/ATEC SERIES ROUND: 133

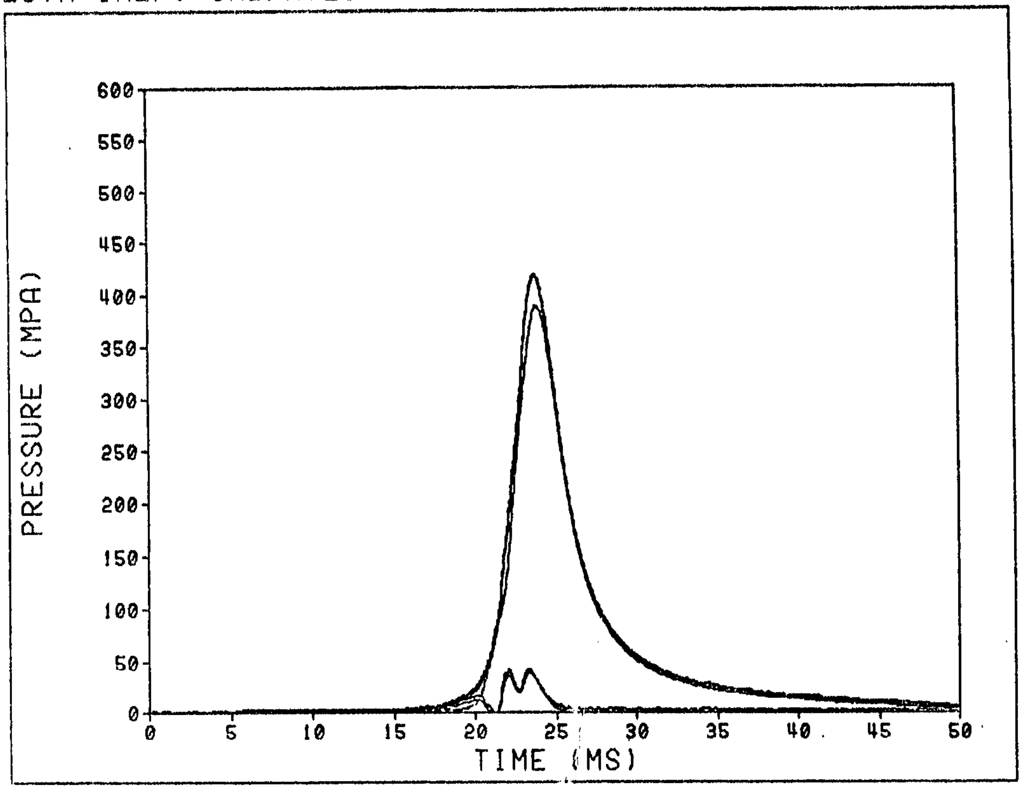

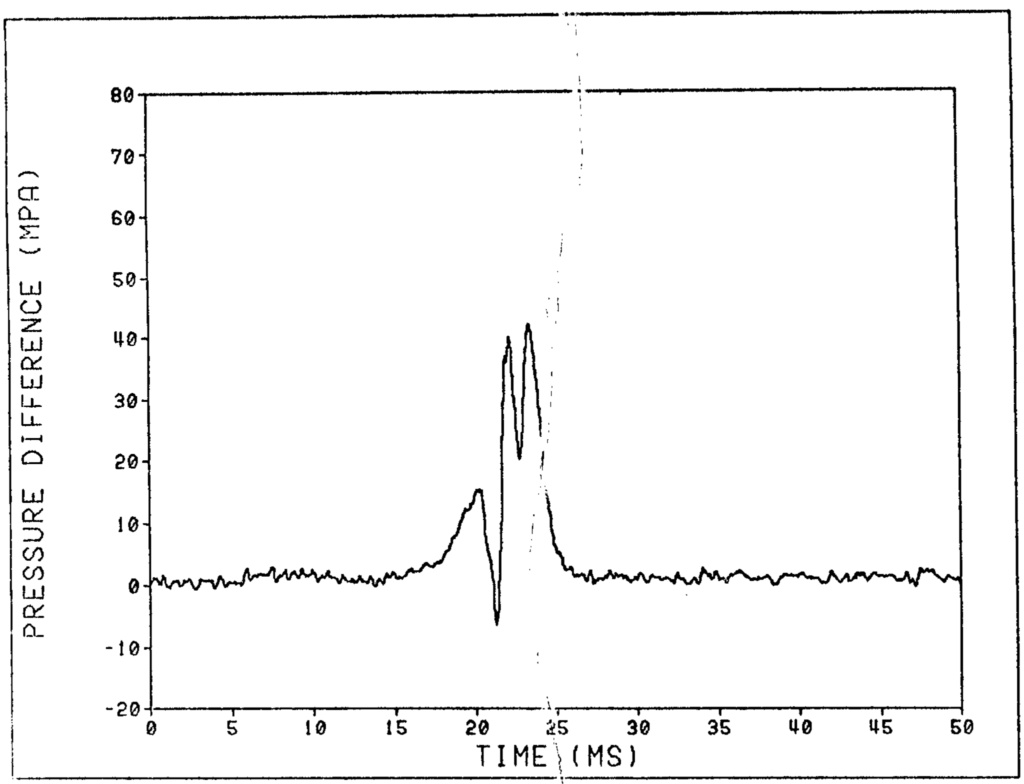

LOVA-IHEP: CAB/ATEC SERIES ROUND: 134

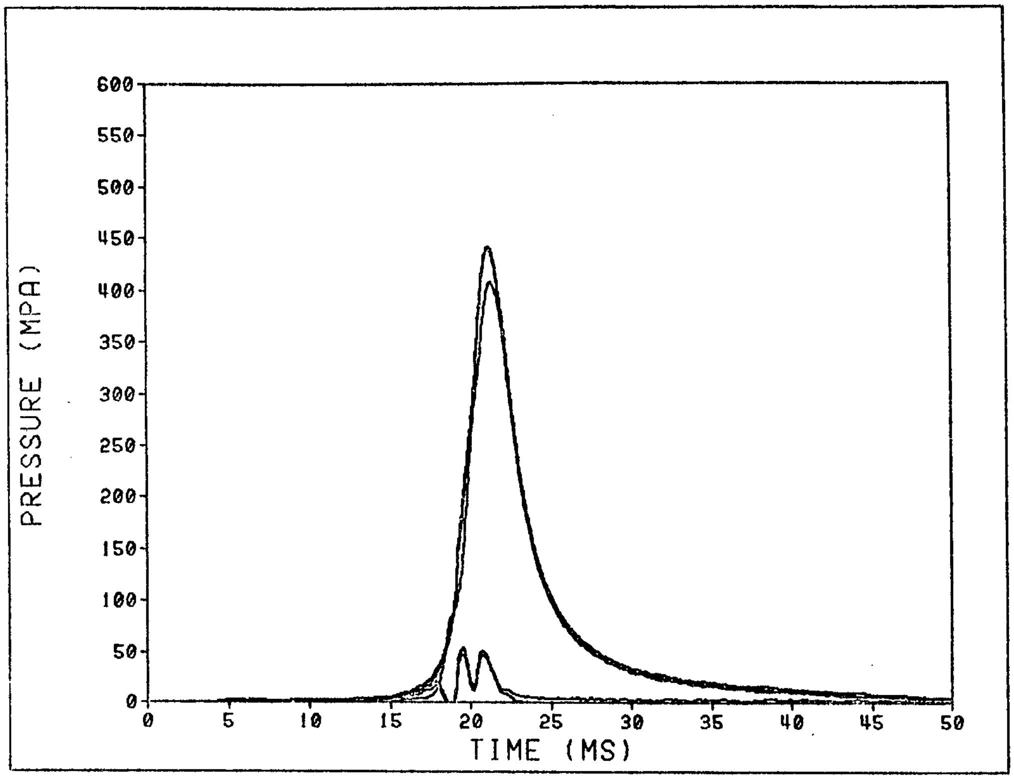

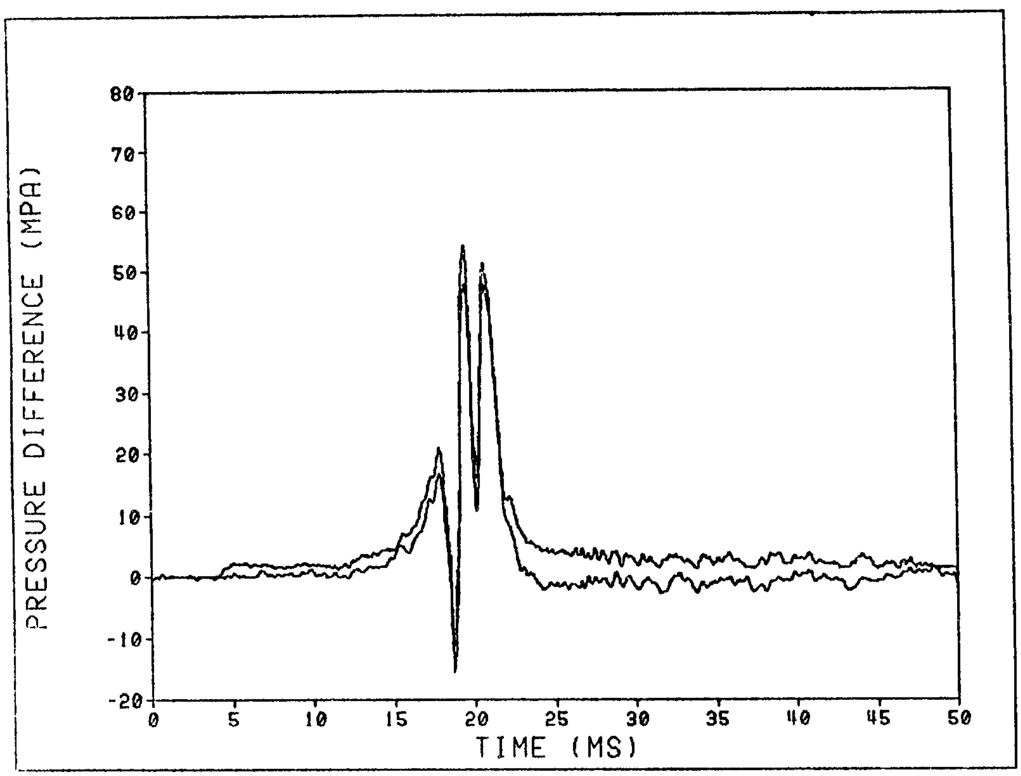

LOVA-IHEP: CAB/ATEC SERIES ROUND: 135

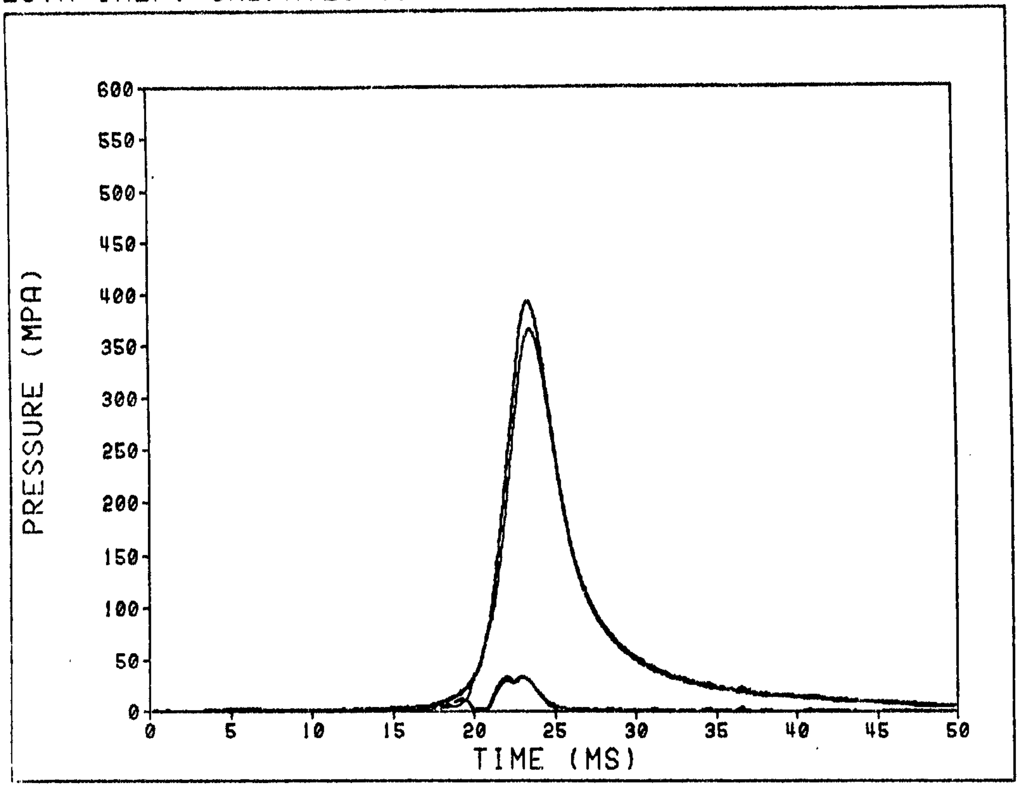

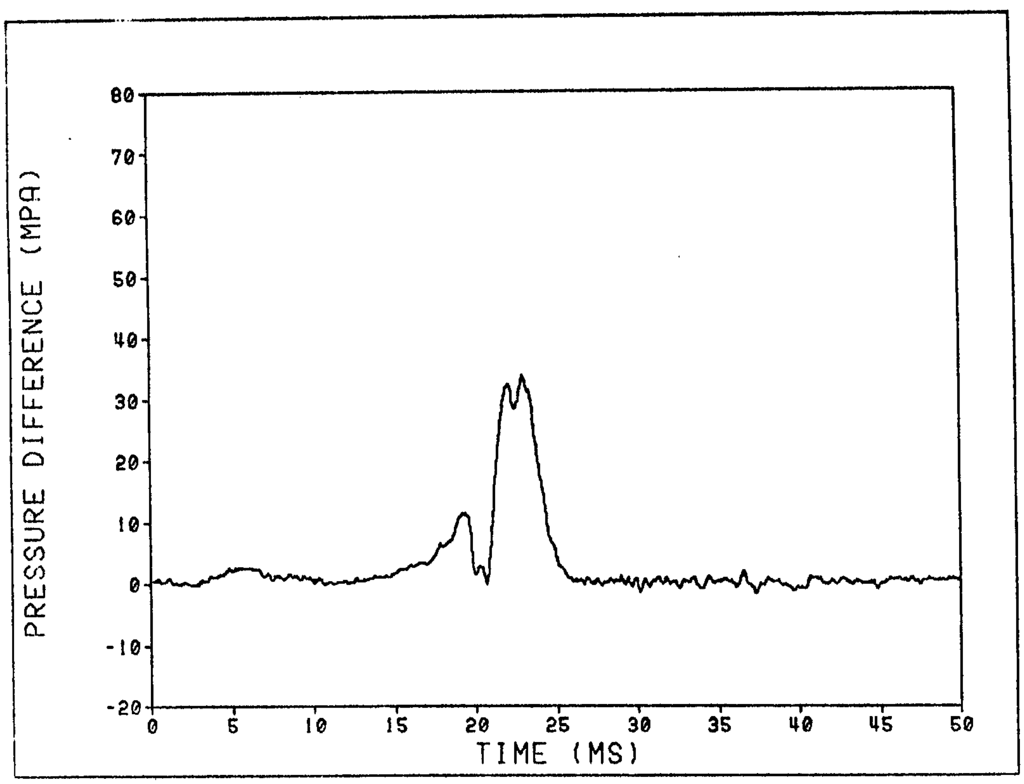

LOVA-IHEP: CAB/ATEC SERIES ROUND: 136

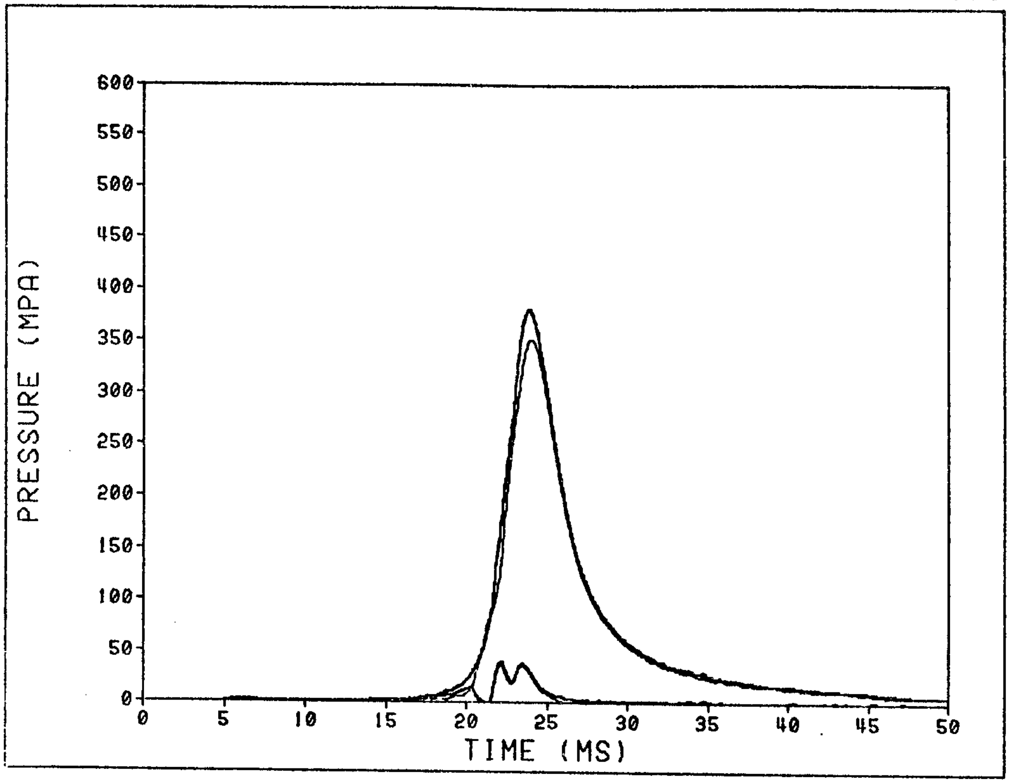

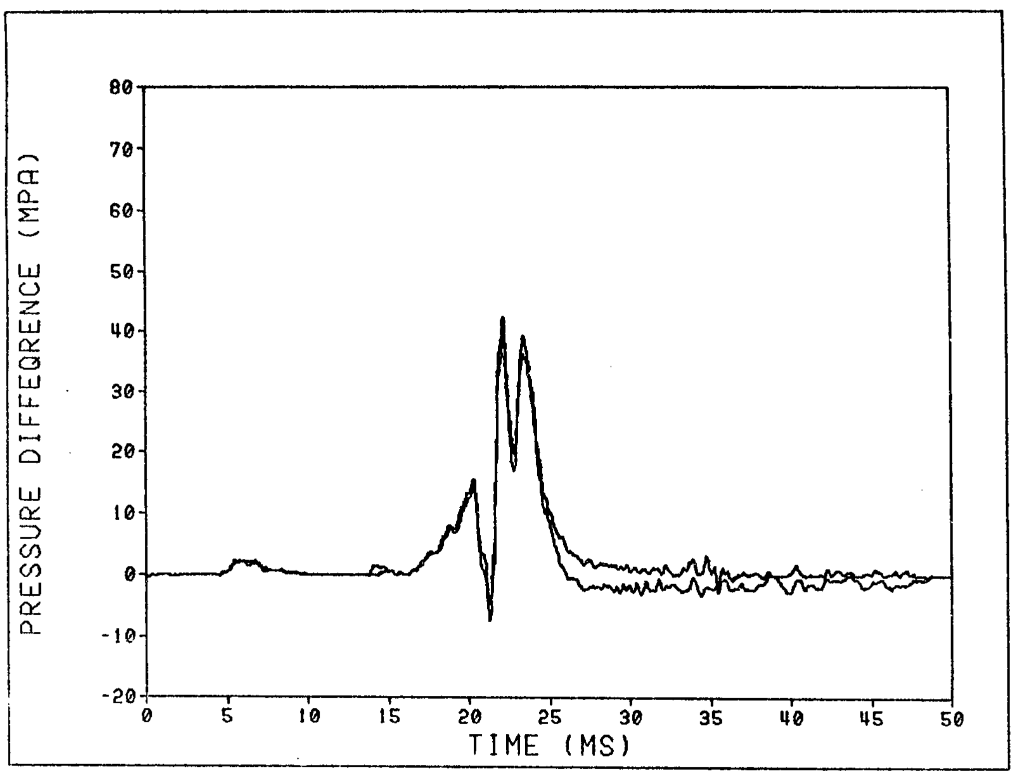

LOVA-IHEP: CAB/ATEC SERIES ROUND: 137

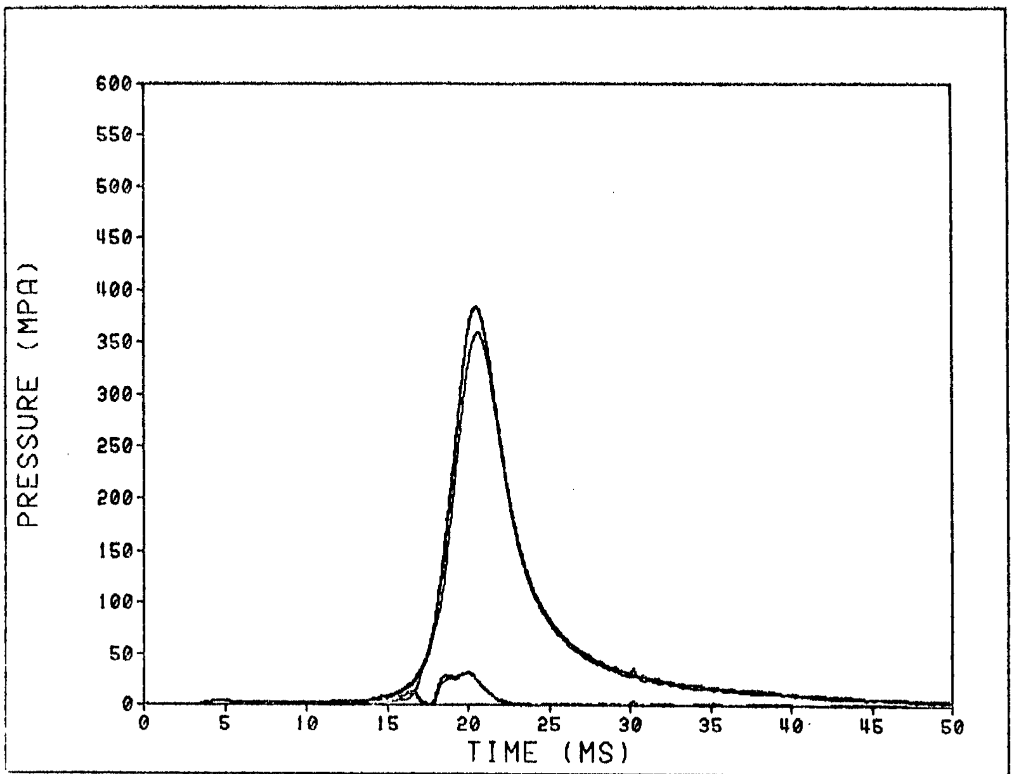

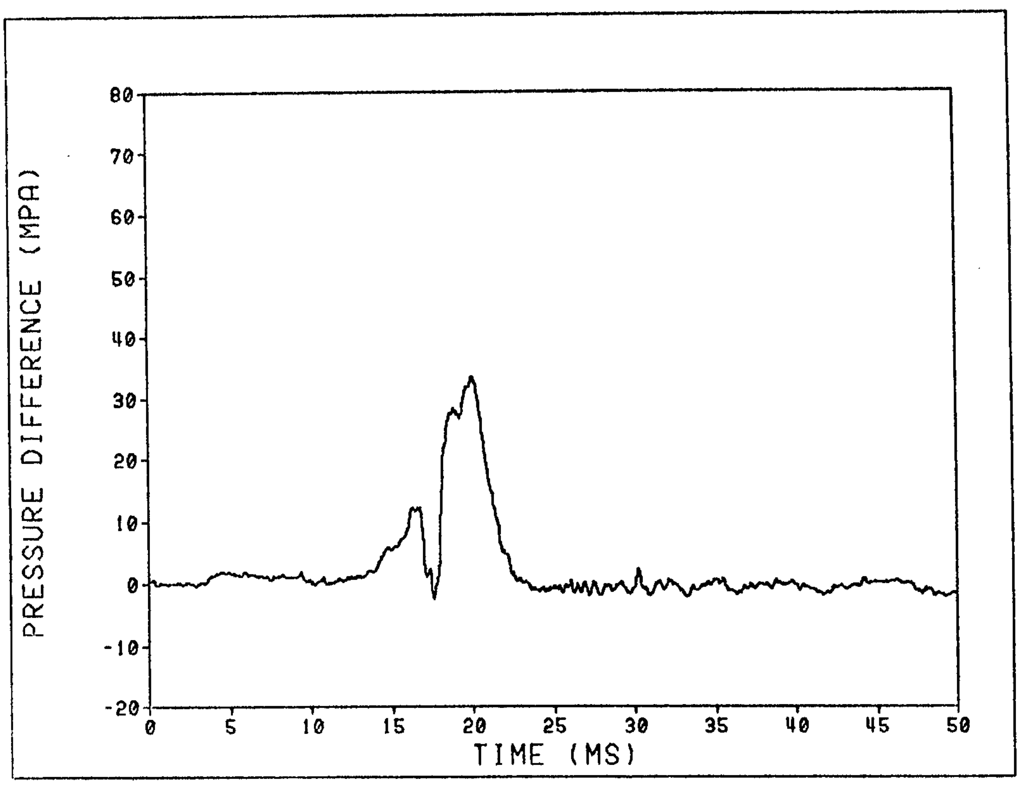

LOVA-IHEP: CAB/ATEC SERIES ROUND: 138

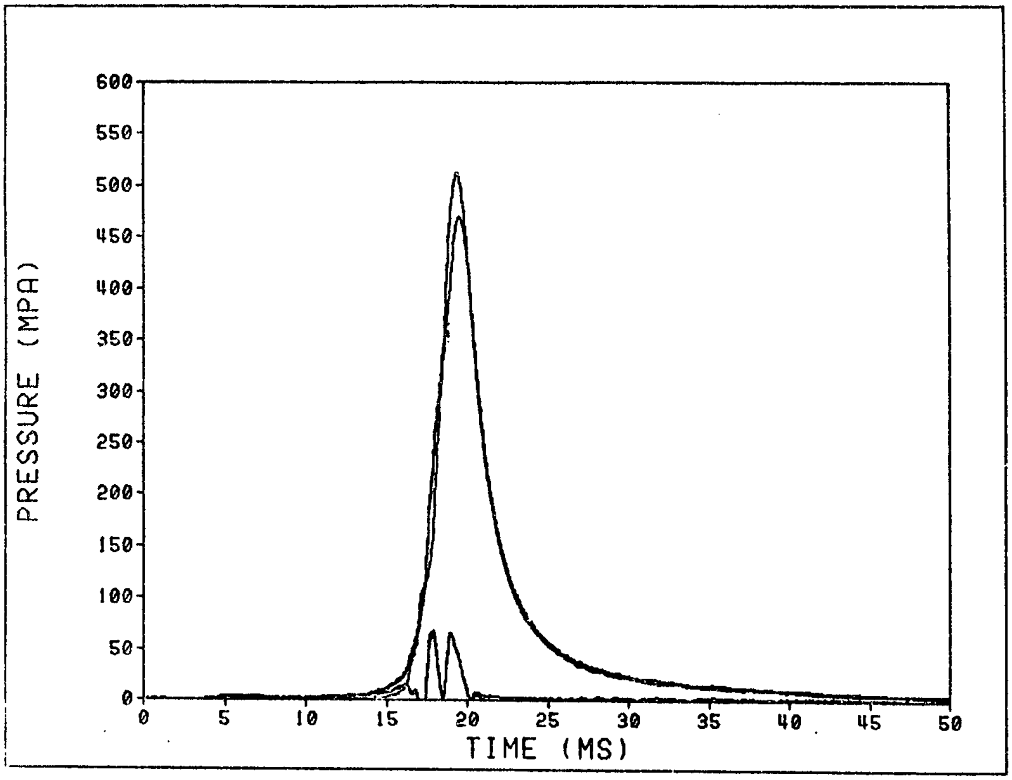

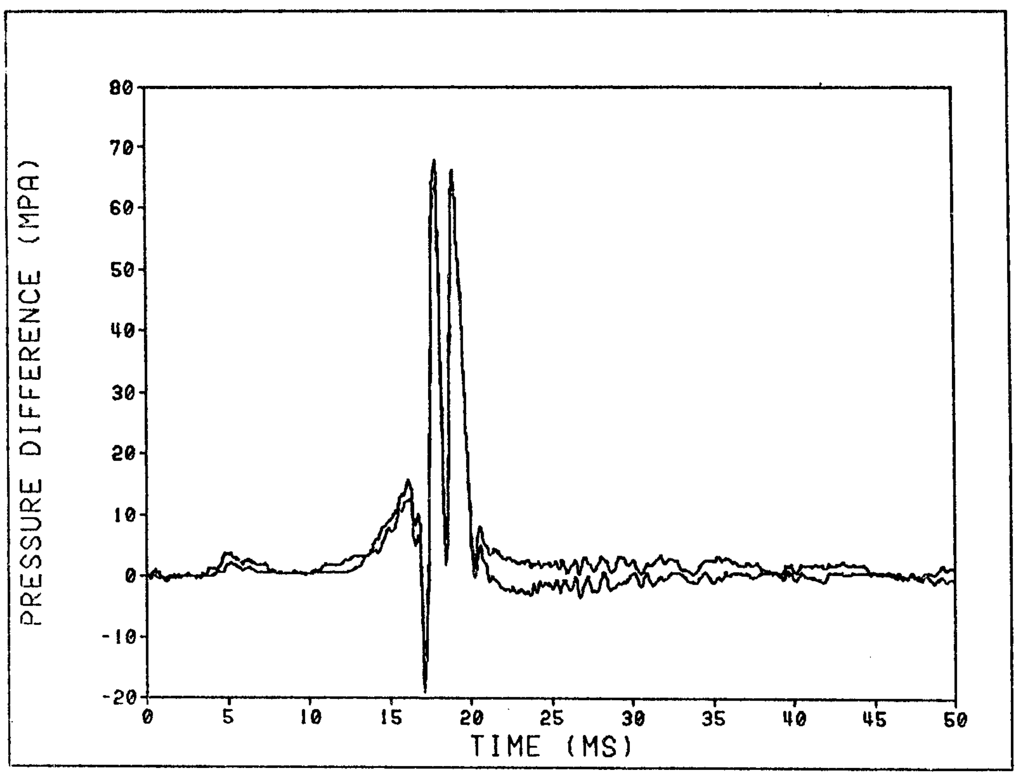

LOVA-IHEP: CAB/ATEC SERIES

ROUND: 139

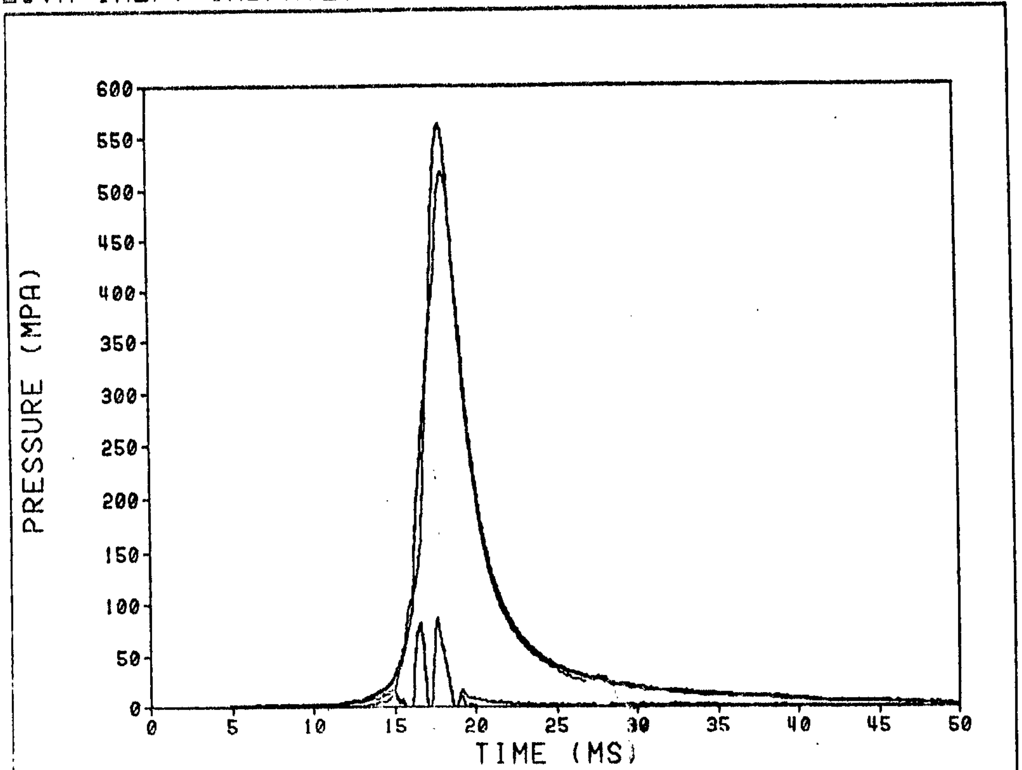

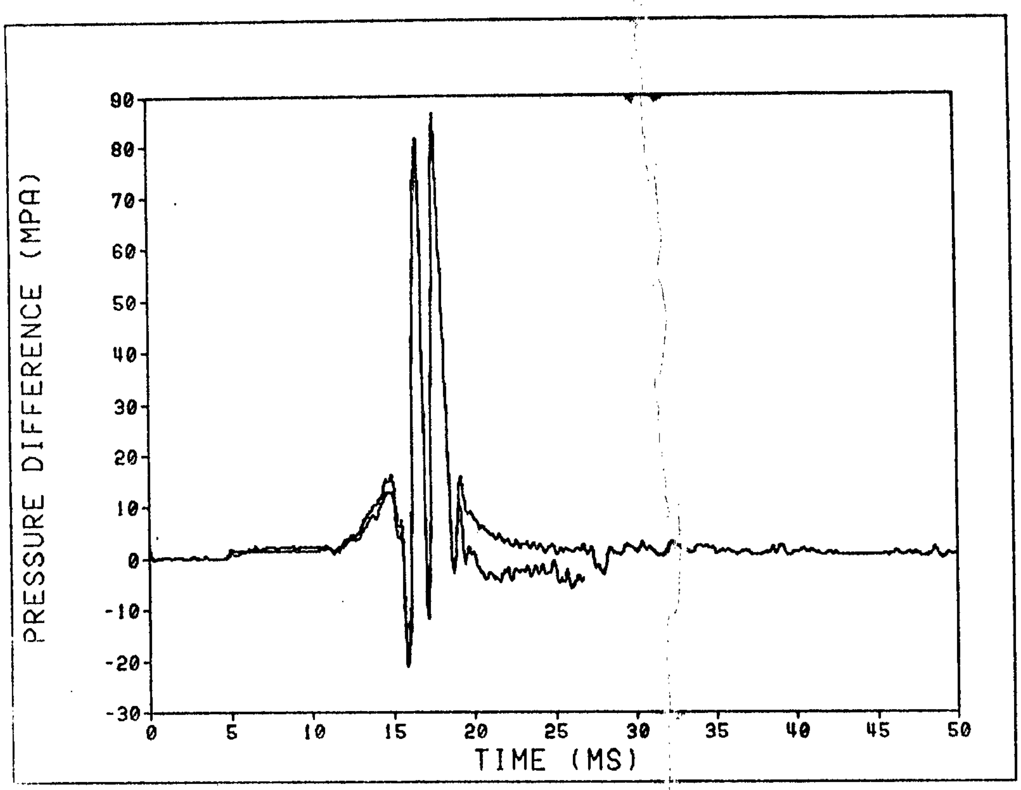

LOVA-IHEP: CAB/ATEC SERIES ROUND: 140

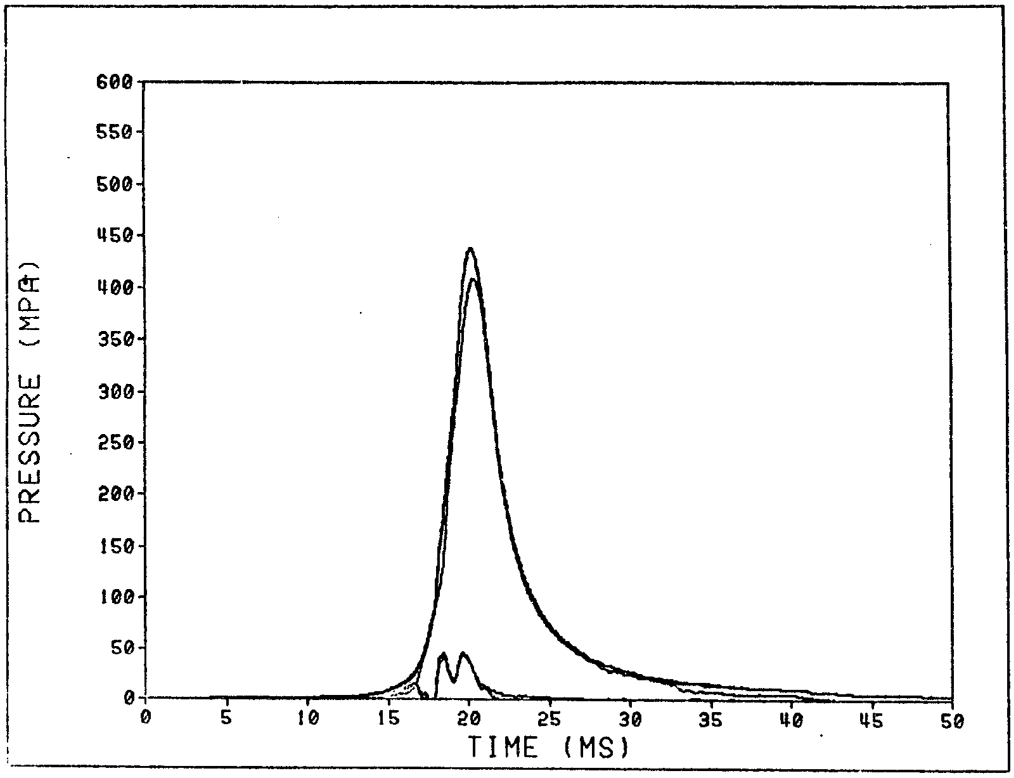

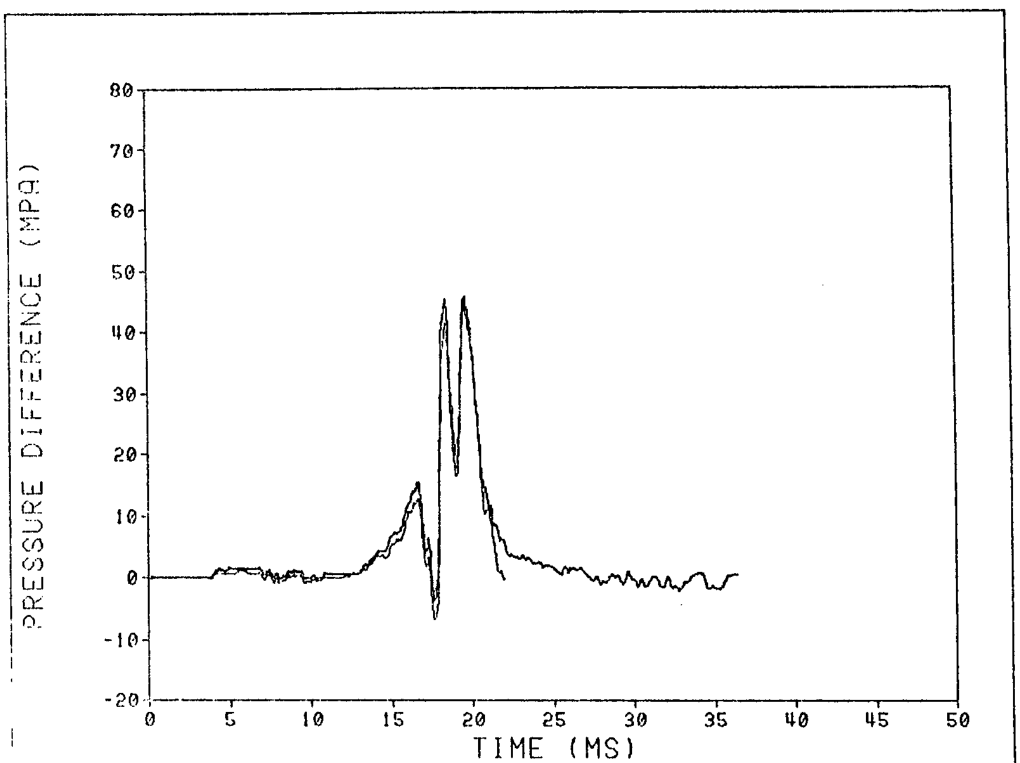

APPENDIX B

NOVA SIMULATIONS OF PRESSURE DIFFERENCE VERSUS TIME

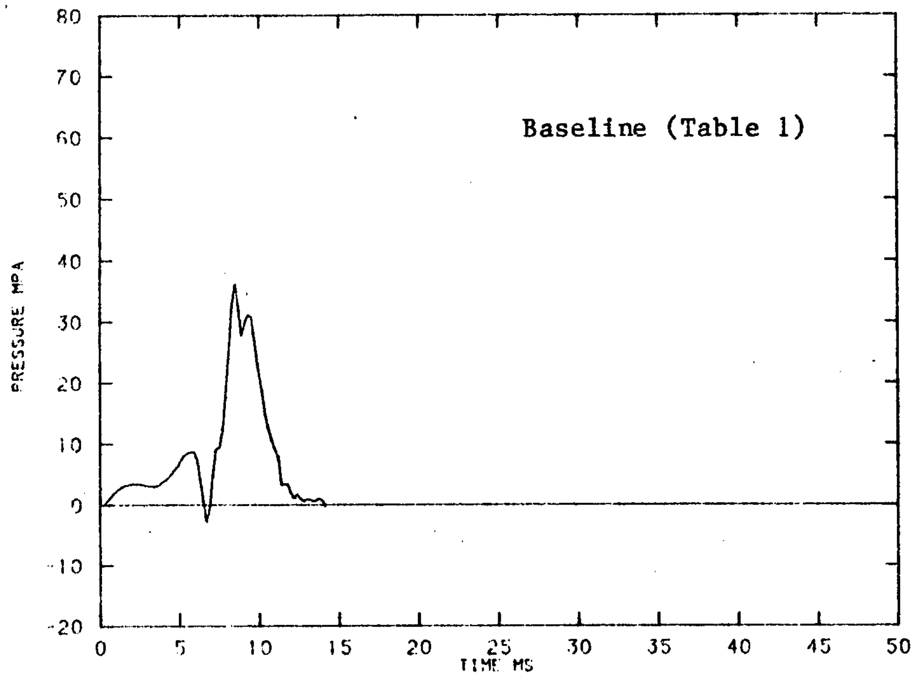
Baseline (Table 1)
PRESSURE MPA
TIME MS

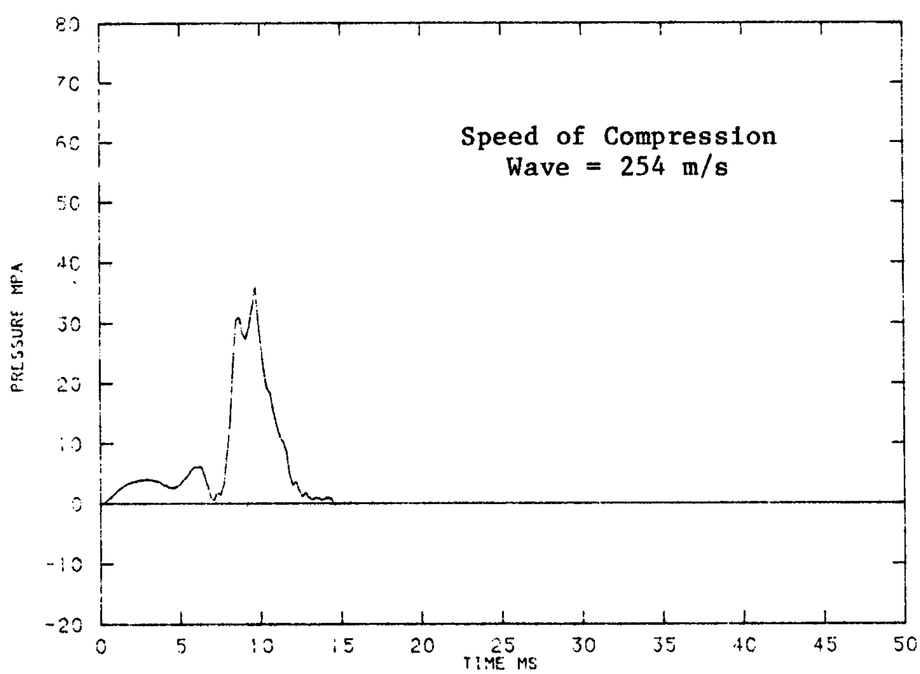
Speed of Compression
Wave = 254 m/s
PRESSURE MPA
TIME MS

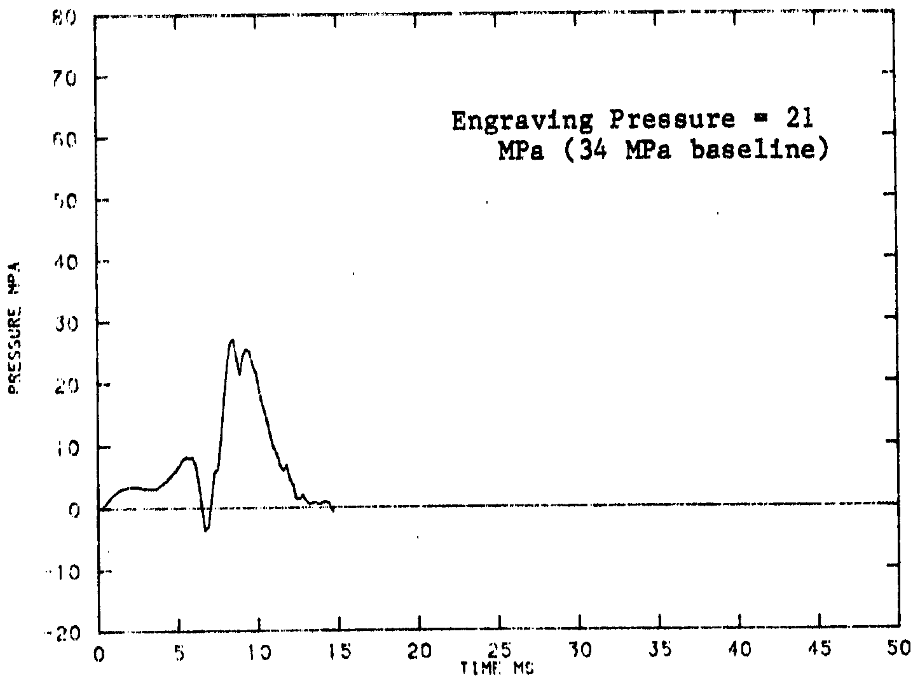

Engraving Pressure = 21
MPa (34 MPa baseline)
PRESSURE MPA
TIME MS

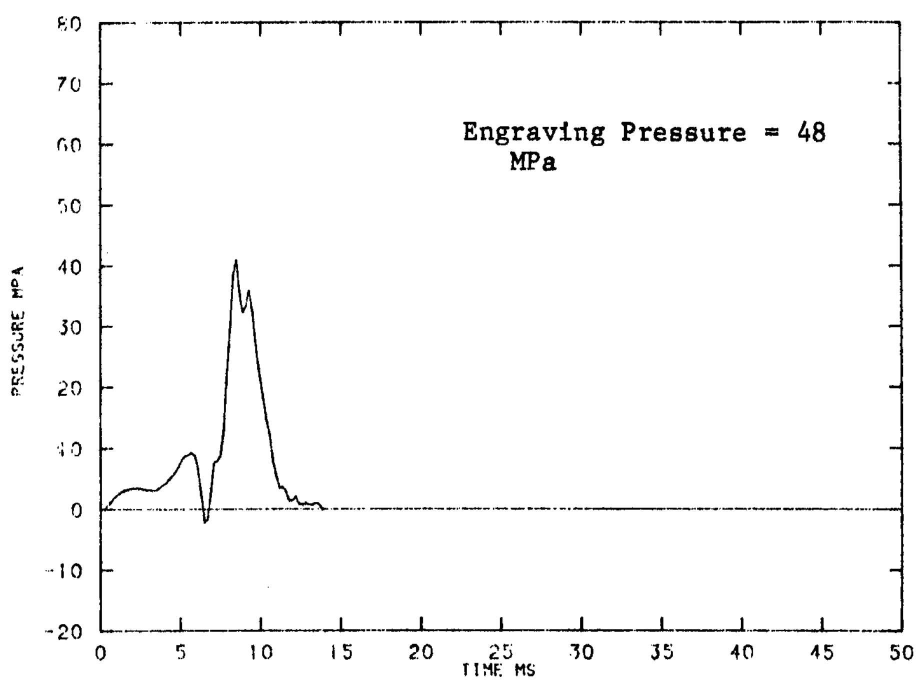

Engraving Pressure = 48
MPa
PRESSURE MPA
TIME MS

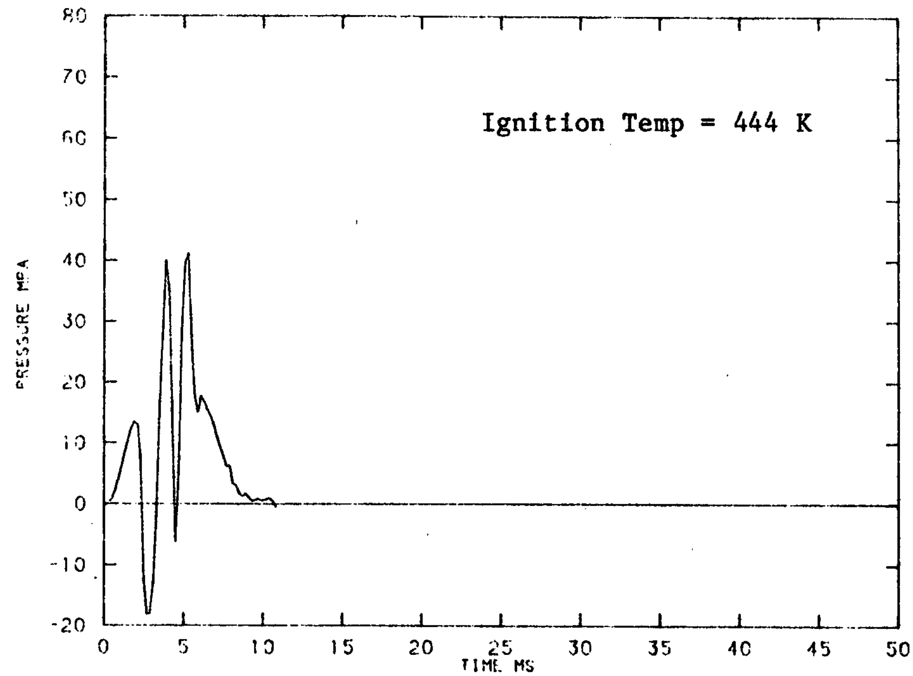
Ignition Temp = 444 K
PRESSURE MPA
TIME MS
80
70
60
50
40
30
20
10
0
-10
-20
0
5
10
15
20
25
30
35
40
45
50

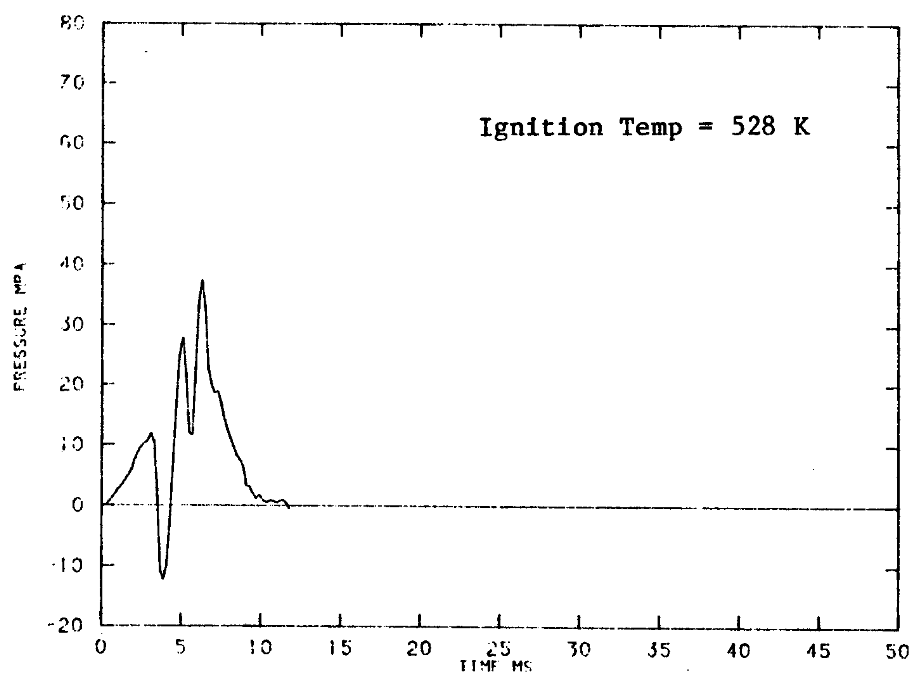
Ignition Temp = 528 K
PRESSURE MPA
TIME MS
80
70
60
50
40
30
20
10
0
-10
-20
0
5
10
15
20
25
30
35
40
45
50

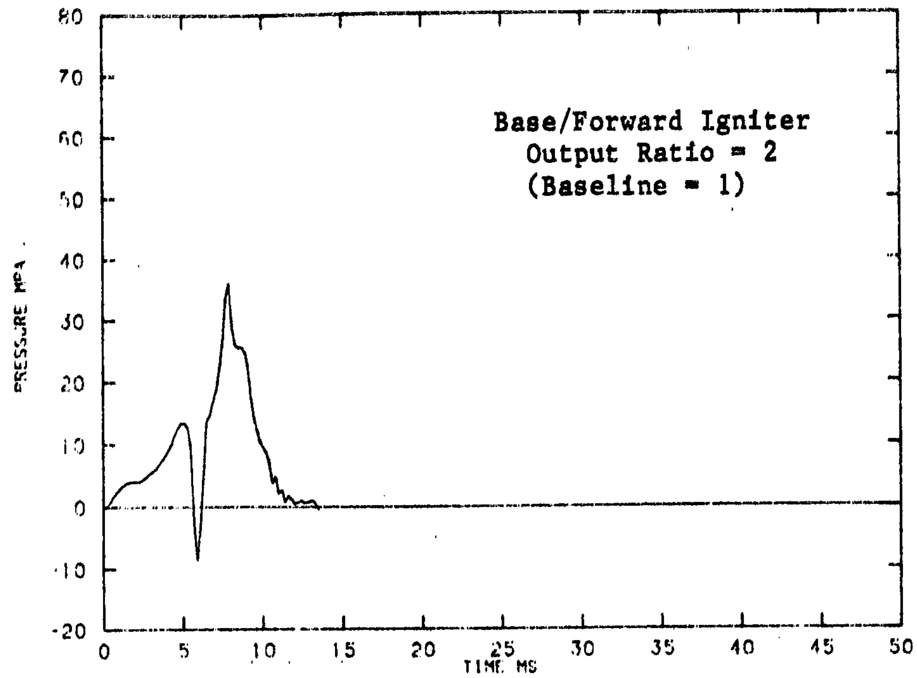
Base/Forward Igniter
Output Ratio = 2
(Baseline = 1)
PRESSURE MPA
TIME, MS

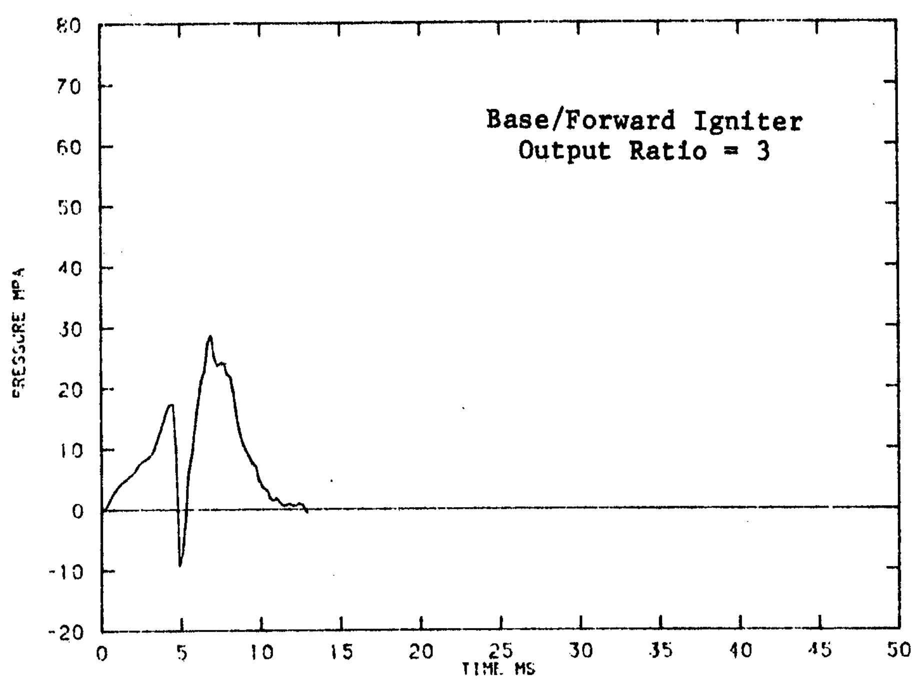
Base/Forward Igniter
Output Ratio = 3
PRESSURE MPA
TIME, MS

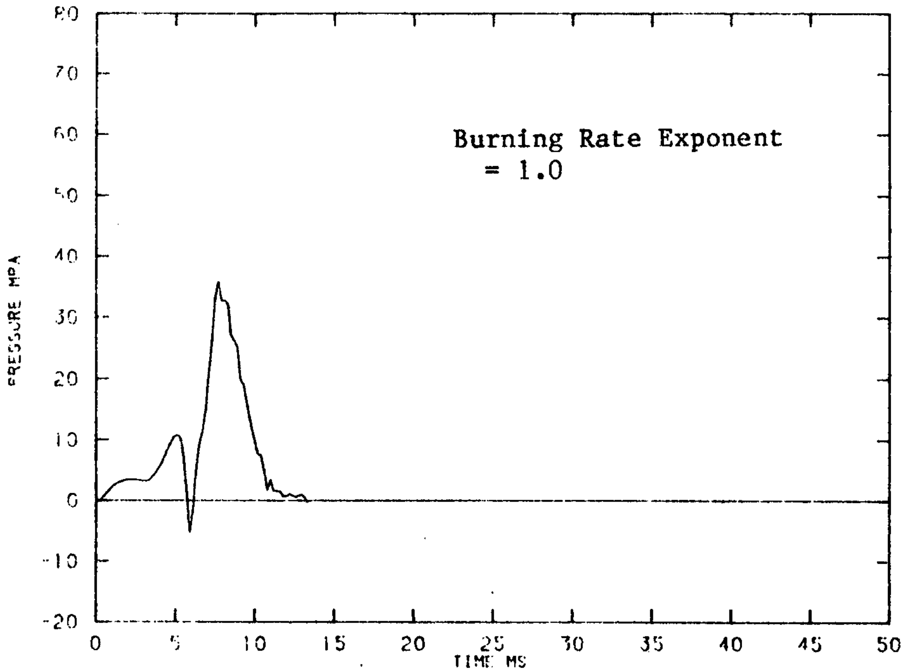
Burning Rate Exponent
= 1.0
PRESSURE MPA
TIME MS

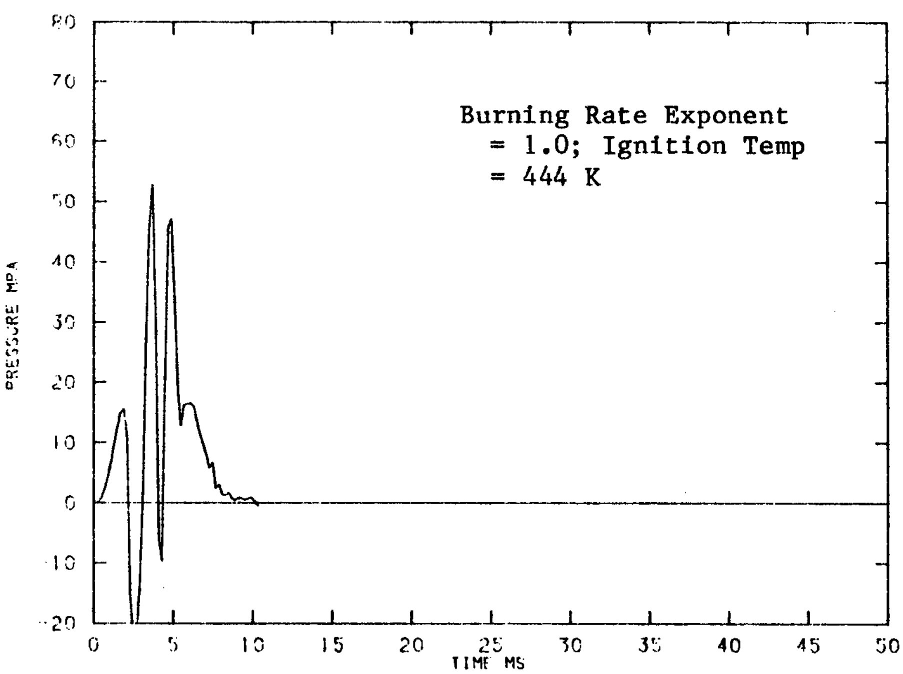
Burning Rate Exponent
= 1.0; Ignition Temp
= 444 K
PRESSURE MPA
TIME MS

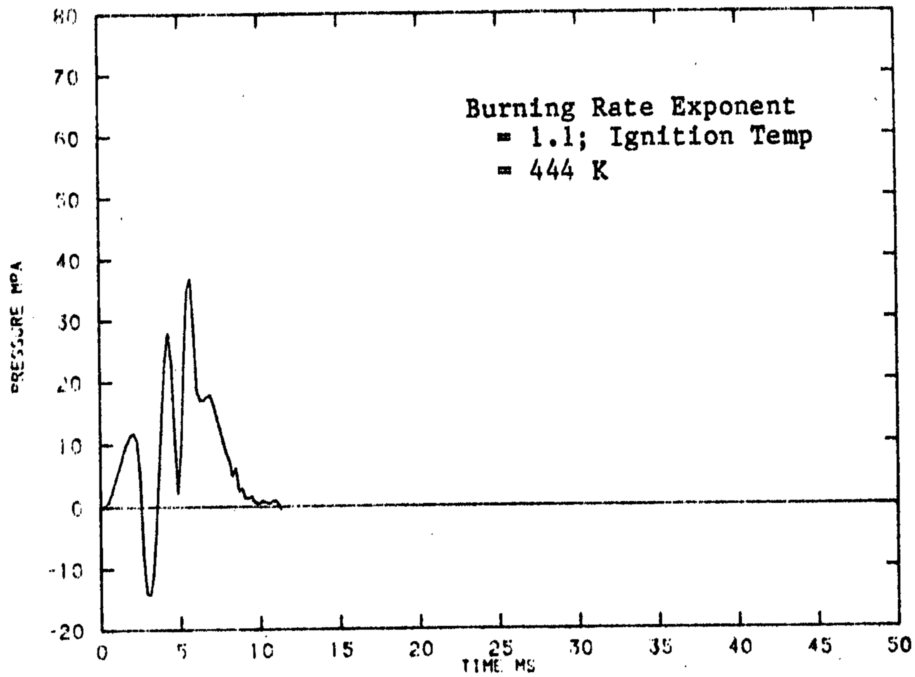
Burning Rate Exponent
= 1.1; Ignition Temp
= 444 K
PRESSURE MPA
TIME MS
80
70
60
50
40
30
20
10
0
-10
-20
0
5
10
15
20
25
30
35
40
45
50

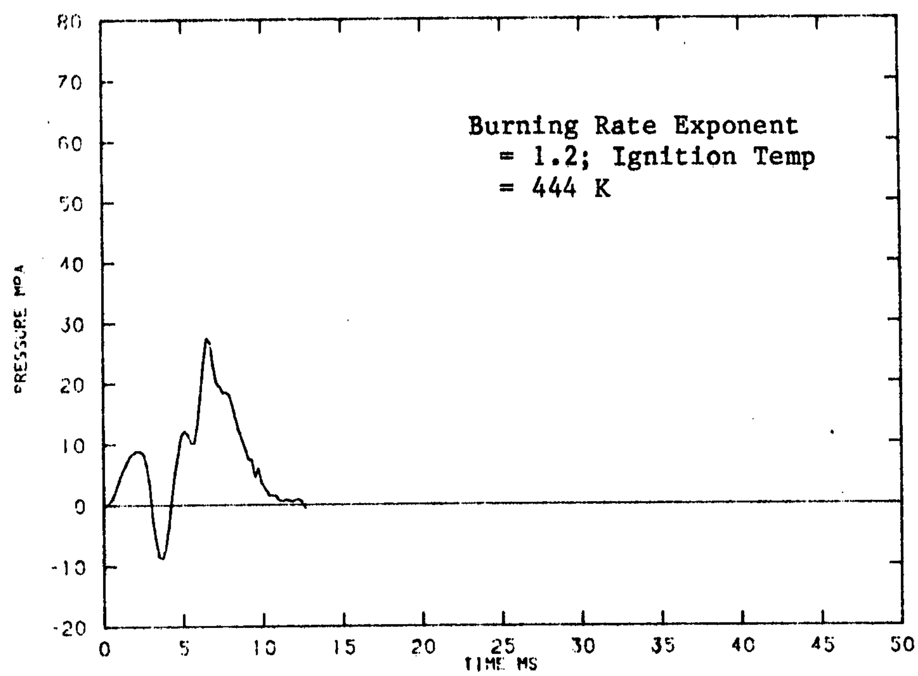
Burning Rate Exponent
= 1.2; Ignition Temp
= 444 K
PRESSURE MPA
TIME MS
80
70
60
50
40
30
20
10
0
-10
-20
0
5
10
15
20
25
30
35
40
45
50

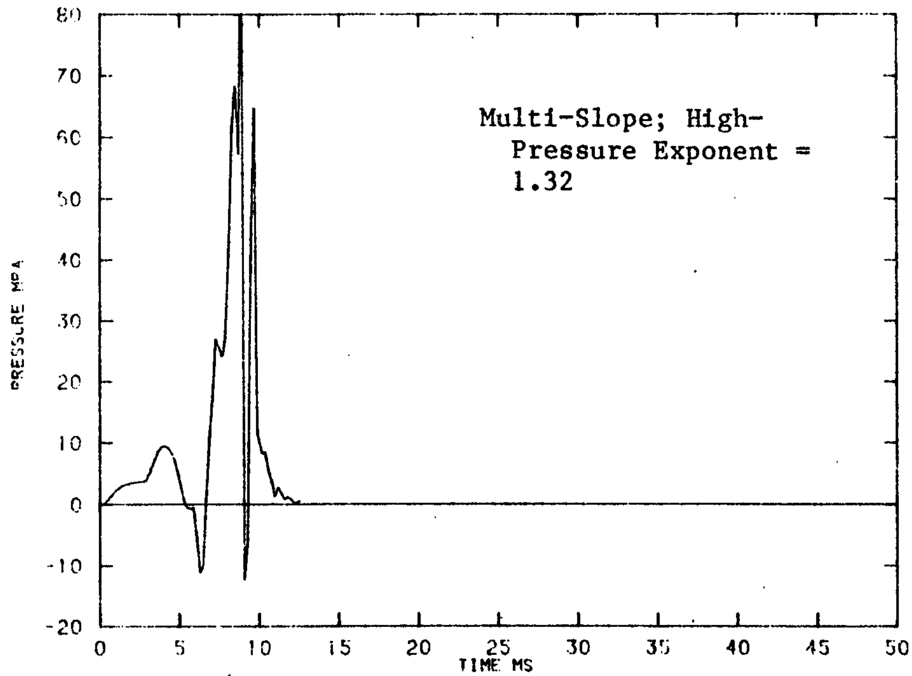
Multi-Slope; High-
Pressure Exponent =
1.32
PRESSURE MPA
TIME MS
80
70
60
50
40
30
20
10
0
-10
-20
0
5
10
15
20
25
30
35
40
45
50

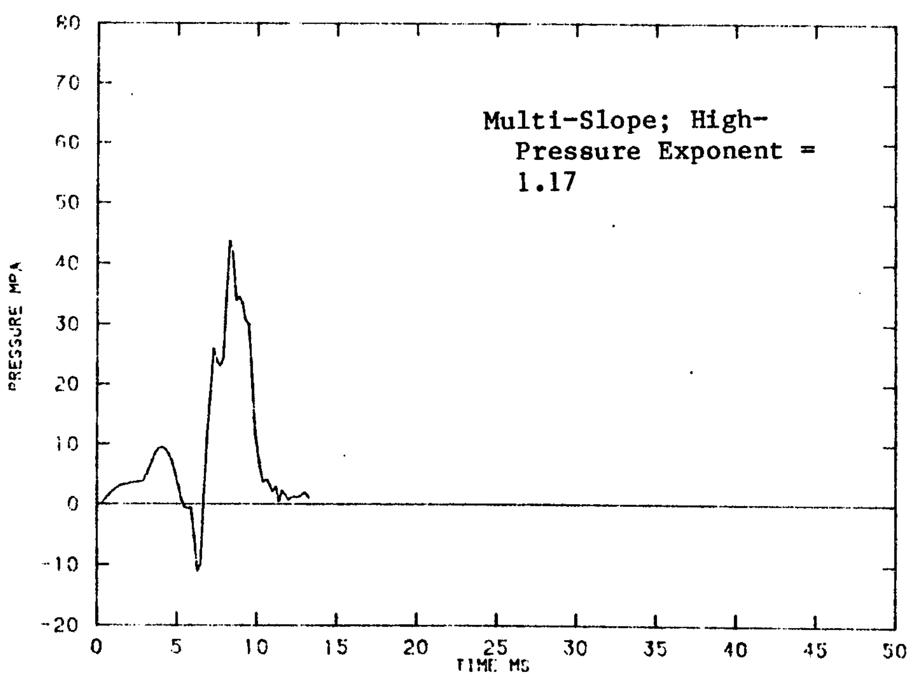
Multi-Slope; High-
Pressure Exponent =
1.17
PRESSURE MPA
TIME MS
80
70
60
50
40
30
20
10
0
-10
-20
0
5
10
15
20
25
30
35
40
45
50

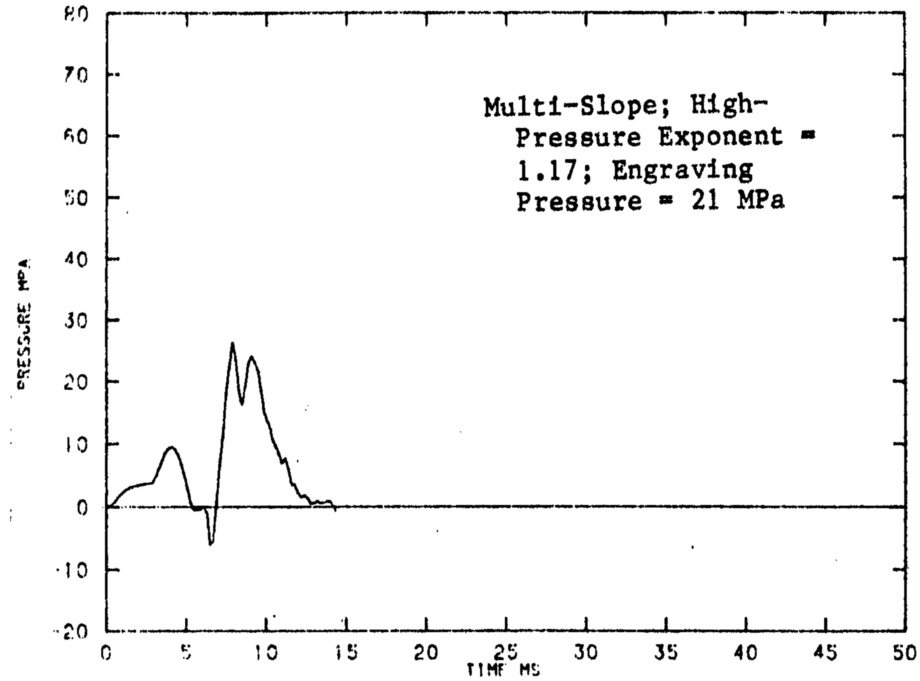

Multi-Slope; High-Pressure Exponent = 1.17; Engraving Pressure = 21 MPa
PRESSURE MPA
TIME MS
80
70
60
50
40
30
20
10
0
-10
-20
0
5
10
15
20
25
30
35
40
45
50

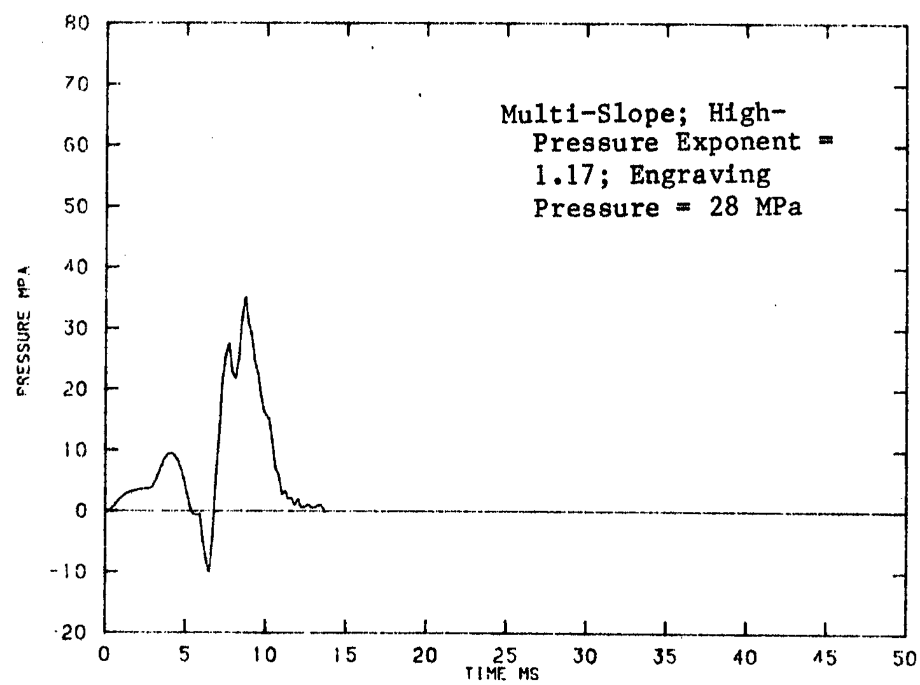

Multi-Slope; High-Pressure Exponent = 1.17; Engraving Pressure = 28 MPa
PRESSURE MPA
TIME MS
80
70
60
50
40
30
20
10
0
-10
-20
0
5
10
15
20
25
30
35
40
45
50

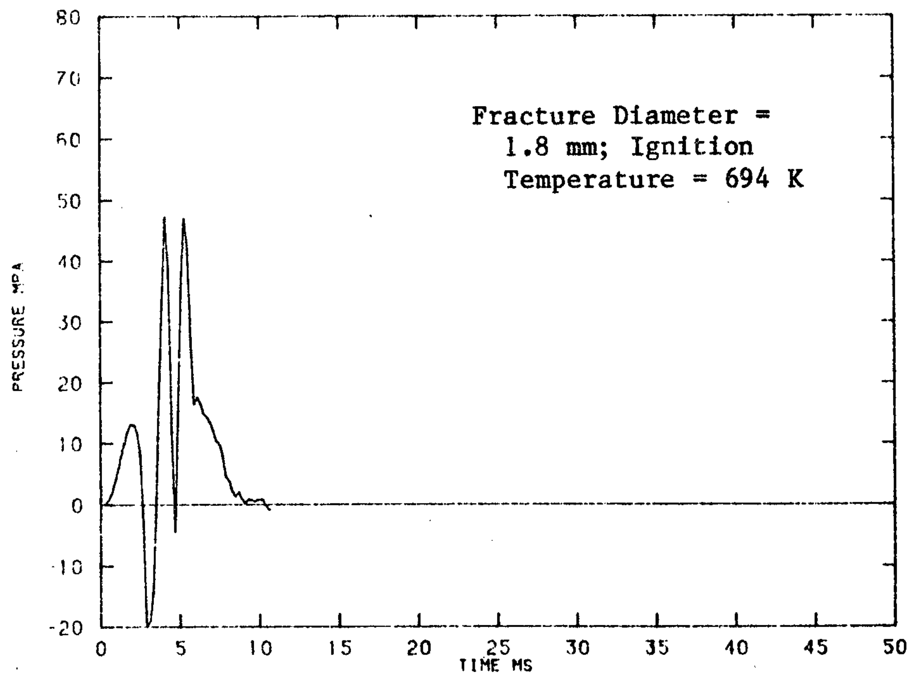
Fracture Diameter =
1.8 mm; Ignition
Temperature = 694 K
PRESSURE MPA
TIME MS
80
70
60
50
40
30
20
10
0
-10
-20
0
5
10
15
20
25
30
35
40
45
50

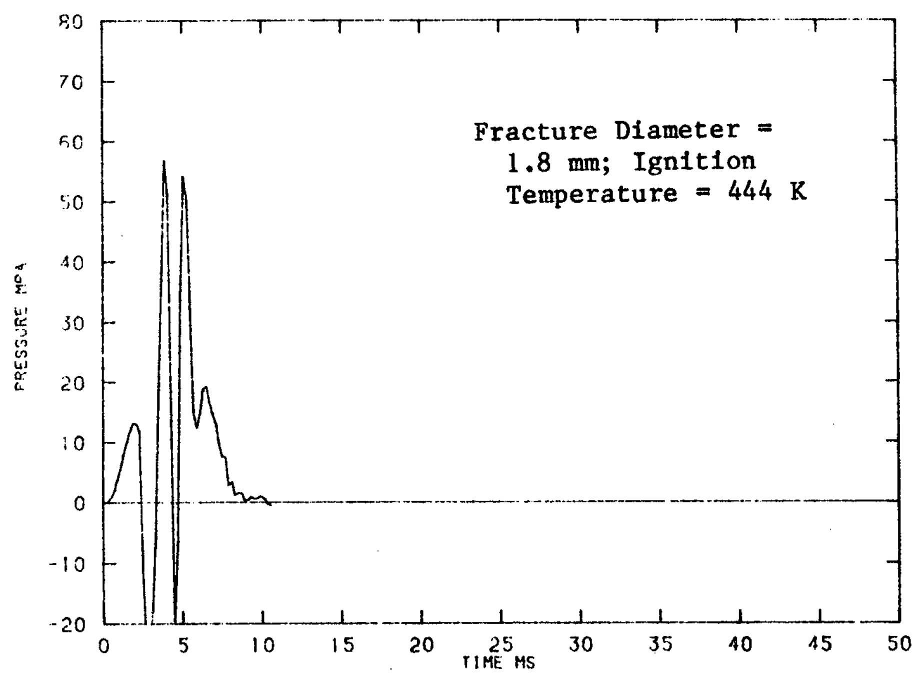
Fracture Diameter =
1.8 mm; Ignition
Temperature = 444 K
PRESSURE MPA
TIME MS
80
70
60
50
40
30
20
10
0
-10
-20
0
5
10
15
20
25
30
35
40
45
50

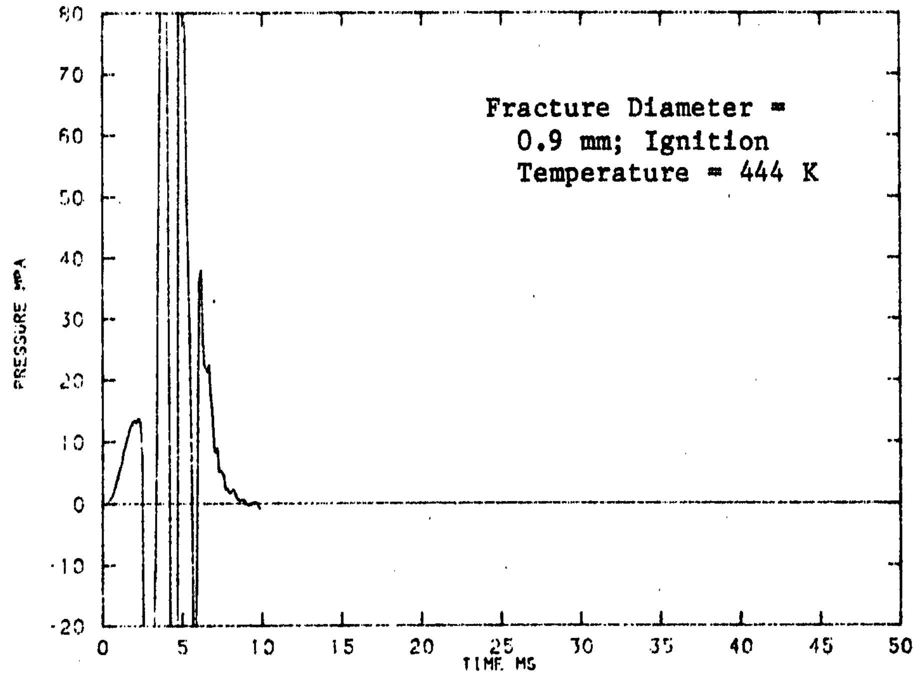
Fracture Diameter =
0.9 mm; Ignition
Temperature = 444 K
PRESSURE MPA
TIME MS
80
70
60
50
40
30
20
10
0
-10
-20
0
5
10
15
20
25
30
35
40
45
50

DISTRIBUTION LIST

No. Of Copies	Organization
12	Administrator Defense Technical Info Center ATTN: DTIC-DDA Cameron Station Alexandria, VA 22314
1	Office of the Under Secretary of Defense Research & Engineering ATTN: R. Thorkildsen Washington, DC 20301
1	HQDA/SAUS-OR, D. Hardison Washington, DC 20301
1	HQDA/DAMA-ZA Washington, DC 20310
1	HQDA, DAMA-CSM, E. Lippi Washington, DC 20310
1	HQDA/SARDA Washington, DC 20310
1	Commandant US Army War College ATTN: Library-FF229 Carlisle Barracks, PA 17013
1	Commander Ballistic Missile Defense Advanced Technology Center P. O. Box 1500 Huntsville, AL 35804
1	Chairman DOD Explosives Safety Board Room 856-C Hoffman Bldg. 1 2461 Eisenhower Avenue Alexandria, VA 22331
3	Commander US Army Materiel Development and Readiness Command ATTN: DRCDMD-ST DRCSF-E, Safety Office DRCDE-DW 5001 Eisenhower Avenue Alexandria, VA 22333
14	Commander US Army Armament R&D Command ATTN: DRDAR-TD, A. Moss DRDAR-TSS DRDAR-TCD Dr. D. Gyorog DRDAR-LCA K. Russell J. Lannon A. Beardell D. Downs S. Einstein L. Schlosberg S. Westley S. Bernstein P. Kemmey C. Heyman Dover, NJ 07801
9	US Army Armament R&D Command ATTN: DRDAR-SCA, L. Stiefel B. Brodman DRDAR-LCB-I, D. Spring DRDAR-LCE, R. Walker DRDAR-LCU-CT E. Barrieres R. Davitt DRDAR-LCU-CV C.Mandala E. Moore DRDAR-LCM-E S. Kaplowitz Dover, NJ 07801

DISTRIBUTION LIST

No. Of Copies	Organization
1	Commander US Army Armament R&D Command ATTN: DRDAR-QAR, J. Rutkowski Dover, NJ 07801
5	Project Manager Cannon Artillery Weapons System ATTN: DRCPM-CW, F. Menke DRCPM-CWW H. Noble DRCPM-CWS M. Fisette DRCPM-CWA R. DeKleine H. Hassmann Dover, NJ 07801
2	Project Manager Munitions Production Base Modernization and Expansion ATTN: DRCPM-PMB, A. Siklosi SARPM-PBM-E, L. Laibson Dover, NJ 07801
3	Project Manager Tank Main Armament System ATTN: DRCPM-TMA, D. Appling DRCPM-TMA-105 DRCPM-TMA-120 Dover, NJ 07801
3	Commander US Army Armament R&D Command ATTN: DRDAR-LCW-A M.Salsbury DRDAR-LCS DRDAR-LC, J. Frasier Dover, NJ 07801
5	Commander US Army Armament Materiel Readiness Command ATTN: DRSAR-LEP-L DRSAR-LC, L. Ambrosini DRSAR-IRC, G. Cowan DRSAR-LEM-W. Fortune R. Zastrow Rock Island, IL 61299
1	Commander US Army Watervliet Arsenal ATTN: SARWV-RD, R. Thierry Watervliet, NY 12189
1	Director US Army ARRADCOM Benet Weapons Laboratory ATTN: DRDAR-LCB-TL Watervliet, NY 12189
1	Commander US Army Aviation Research and Development Command ATTN: DRDAV-E 4300 Goodfellow Blvd. St. Louis, MO 63120
1	Commander US Army TSARCOM 4300 Goodfellow Blvd St. Louis, MO 63120
1	Director US Army Air Mobility Research And Development Laboratory Ames Research Center Moffett Field, CA 94035

DISTRIBUTION LIST

No. Of Copies	Organization
1	Commander US Army Communications Research and Development Command ATTN: DRSEL-ATDD Fort Monmouth, NJ 07703
1	Commander US Army Electronics Research and Development Command Technical Support Activity ATTN: DELSD-L Fort Monmouth, NJ 07703
1	Commander US Army Harry Diamond Lab. ATTN: DELHD-TA-L 2800 Powder Mill Road Adelphi, MD 20783
2	Commander US Army Missile Command ATTN: DRSMI-R DRSMI-YDL Redstone Arsenal, AL 35898
1	Commander US Army Natick Research and Development Command ATTN: DRDNA-DT, D. Sieling Natick, MA 01762
1	Commander US Army Tank Automotive Command ATTN: DRSTA-TSL Warren, MI 48090
1	US Army Tank Automotive Materiel Readiness Command ATTN: DRSTA-CG Warren, MI 48090
2	Commandant US Army Infantry School ATTN: ATSH-CD-CSO-OR Fort Benning, GA 31905
1	Project Manager Improved TOW Vehicle ATTN: DRCPM-ITV US Army Tank Automotive Command Warren, MI 48090
1	Program Manager M1 Tank System ATTN: DRCPM-GMC-SA Warren, MI 48090
1	Project Manager Fighting Vehicle Systems ATTN: DRCPM-FVS Warren, MI 48090
1	Director US Army TRADOC Systems Analysis Activity ATTN: ATAA-SL White Sands Missile Range NM 88002
1	Project Manager M-60 Tank Development ATTN: DRCPM-M60TD Warren, MI 48090
1	Commander US Army Training & Doctrine Command ATTN: ATCD-MA/ MAJ Williams Fort Monroe, VA 23651
2	Commander US Army Materials and Mechanics Research Center ATTN: DRXMR-ATL Tech Library Watertown, MA 02172

DISTRIBUTION LIST

No. Of Copies	Organization
1	Commander US Army Research Office ATTN: Tech Library P. O. Box 12211 Research Triangle Park, NC 27709
1	Commander US Army Mobility Equipment Research & Development Command ATTN: DRDME-WC Fort Belvoir, VA 22060
1	Commander US Army Logistics Mgmt Ctr Defense Logistics Studies Fort Lee, VA 23801
2	Commandant US Army Infantry School ATTN: Infantry Agency Fort Benning, GA 31905
1	US Army Armor & Engineer Board ATTN: STEBB-AD-S Fort Knox, KY 40121
1	Commandant US Army Aviation School ATTN: Aviation Agency Fort Rucker, AL 36360
1	Commandant Command and General Staff College Fort Leavenworth, KS 66027
1	Commandant US Army Special Warfare School ATTN: Rev & Tng Lit Div Fort Bragg, NC 28307
1	Commandant US Army Engineer School ATTN: ATSE-CD Ft. Belvoir, VA 22060
1	Commander US Army Foreign Science & Technology Center ATTN: DRXST-MC-3 220 Seventh Street, NE Charlottesville, VA 22901
1	President US Army Artillery Board Ft. Sill, OK 73504
1	Commandant US Army Field Artillery School ATTN: ATSF-CO-MW, B. Willis Ft. Sill, OK 73503
3	Commandant US Army Armor School ATTN: ATZK-CD-MS M. Falkovitch Armor Agency Fort Knox, KY 40121
1	Chief of Naval Materiel Department of the Navy ATTN: J. Amlie Washington, DC 20360
1	Office of Naval Research ATTN: Code 473, R. S. Miller 800 N. Quincy Street Arlington, VA 22217
2	Commander Naval Sea Systems Command ATTN: SEA-62R, J. W. Murrin R. Beauregard National Center, Bldg. 2 Room 6E08 Washington, DC 20362
1	Commander Naval Air Systems Command ATTN: NAIR-954-Tech Lib Washington, DC 20360

DISTRIBUTION LIST

No. Of Copies	Organization
1	Strategic Systems Project Office Dept. of the Navy Room 901 ATTN: J. F. Kincaid Washington, DC 20376
1	Assistant Secretary of the Navy (R, E, and S) ATTN: R. Reichenbach Room 5E787 Pentagon Bldg. Washington, DC 20350
1	Naval Research Lab Tech Library Washington, DC 20375
5	Commander Naval Surface Weapons Center ATTN: Code G33, J. L. East W. Burrell J. Johndrow Code G23, D. McClure Code DX-21 Tech Lib Dahlgren, VA 22448
2	Commander US Naval Surface Weapons Center ATTN: J. P. Consaga C. Gotzmer Indian Head, MD 20640
4	Commander Naval Surface Weapons Center ATTN: S. Jacobs/Code 240 Code 730 K. Kim/Code R-13 R. Bernecker Silver Spring, MD 20910
2	Commanding Officer Naval Underwater Systems Center Energy Conversion Dept. ATTN: CODE 5B331, R. S. Lazar Tech Lib Newport, RI 02840
4	Commander Naval Weapons Center ATTN: Code 388, R. L. Derr C. F. Price T. Boggs Info. Sci. Div. China Lake, CA 93555
2	Superintendent Naval Postgraduate School Dept. of Mechanical Engineering ATTN: A. E. Fuhs Code 1424 Library Monterey, CA 93940
6	Commander Naval Ordnance Station ATTN: P. L. Stang J. Birkett S. Mitchell C. Christensen D. Brooks Tech Library Indian Head, MD 20640
1	AFSC/SDOA Andrews AFB Washington, DC 20334
1	AFOSR Directorate of Aerospace Sciences ATTN: L. H. Caveny Bolling AFB, DC 20332
6	AFRPL (DYSC) ATTN: D. George J. N. Levine B. Goshgarian D. Thrasher N. Vander Hyde Tech Library Edwards AFB, CA 93523

DISTRIBUTION LIST

No. Of Copies	Organization
1	AFFTC ATTN: SSD-Tech LIb Edwards AFB, CA 93523
1	AFATL ATTN: DLYV Eglin AFB, FL 32542
1	AFATL/DLDL ATTN: O. K. Heiney Eglin AFB, FL 32542
1	ADTC ATTN: DLODL Tech Lib Eglin AFB, FL 32542
1	Atlantic Research Corporation ATTN: M. K. King 5390 Cherokee Ave. Alexandria, VA 22314
1	NASA HQ 600 Independence Avenue, SW ATTN: Code JM6, Tech Lib. Washington, DC 20546
1	NASA/Lyndon B. Johnson Space Center ATTN: NHS-22, Library Section Houston, TX 77058
1	Aerodyne Research, Inc. Bedford Research Park ATTN: V. Yousefian Bedford, MA 01730
1	Aerojet Solid Propulsion Co. ATTN: P. Micheli Sacramento, CA 95813

No. Of Copies	Organization
1	AVCO Everett Rsch Lab ATTN: D. Stickler 2385 Revere Beach Parkway Everett, MA 02149
2	Calspan Corporation ATTN: E. B. Fisher Tech Library P. O. Box 400 Buffalo, NY 14225
1	Foster Miller Associates ATTN: A. Erickson 135 Second Avenue Waltham, MD 02154
1	Pulsepower Systems, Inc. ATTN: L. C. Elmore 815 American Street San Carlos, CA 94070
1	General Applied Sciences Lab ATTN: J. Erdos Merrick & Stewart Avenues Westbury Long Island, NY 11590
1	General Electric Company Armament Systems Dept. ATTN: M. J. Bulman, Room 1311 Lakeside Avenue Burlington, VT 05412
1	Hercules Powder Co. Allegheny Ballistics Laboratory ATTN: R. B. Miller P. O. Box 210 Cumberland, MD 21501
1	Hercules, Inc Bacchus Works ATTN: K. P. McCarty P. O. Box 98 Magna, UT 84044

DISTRIBUTION LIST

No. Of Copies	Organization
1	Hercules, Inc. Eglin Operations AFATL DLDL ATTN: R. L. Simmons Eglin AFB, FL 32542
1	IITRI ATTN: M. J. Klein 10 W. 35th Street Chicago, IL 60616
2	Lawrence Livermore Laboratory ATTN: M. S. L-355, A. Buckingham M. Finger P. O. Box 808 Livermore, CA 94550
1	Olin Corporation Badger Army Ammunition Plant ATTN: R. J. Thiede Baraboo, WI 53913
1	Olin Corporation Smokeless Powder Operations ATTN: R. L. Cook P. O. Box 222 ST. Marks, FL 32355
1	Paul Gough Associates, Inc. ATTN: P. S. Gough P. O. Box 1614 Portsmouth, NH 03801
1	Physics International Company 2700 Merced Street Leandro, CA 94577
1	Princeton Combustion Research Lab. ATTN: M. Summerfield 1041 US Highway One North Princeton, NJ 08540
2	Rockwell International Rocketdyne Division ATTN: BA08 J. E. Flanagan J. Grey 6633 Canoga Avenue Canoga Park, CA 91304
1	Science Applications, Inc. ATTN: R. B. Edelman 23146 Cumorah Crest Woodland Hills, CA 91364
1	Scientific Research Assoc., Inc. ATTN: H. McDonald P. O. Box 498 Glastonbury, CT 06033
2	Thikol Corp Elkton Div ATTN: R. Biddle Tech Lib P.O. Box 241 Elkton, MD 21921
3	Thiokol Corporation Huntsville Division ATTN: D. Flanigan R. Glick Tech Library Huntsville, AL 35807
2	Thiokol Corporation Wasatch Division ATTN: J. Peterson Tech Library P. O. Box 524 Brigham City, UT 84302

DISTRIBUTION LIST

No. Of Copies	Organization	No. Of Copies	Organization
2	United Technologies Chemical Systems Division ATTN: R. Brown Tech Library P. O. Box 358 Sunnyvale, CA 94086	1	University of Massachusetts Dept. of Mechanical Engineering ATTN: K. Jakus Amherst, MA 01002
1	Universal Propulsion Company ATTN: H. J. McSpadden Black Canyon Stage 1 Box 1140 Phoenix, AZ 85029	1	University of Minnesota Dept. of Mechanical Engineering ATTN: E. Fletcher Minneapolis, MN 55455
1	Southwest Research Institute Institute Scientists ATTN: Robert E. White 8500 Culebra Road San Antonio, TX 78228	1	Case Western Reserve University Division of Aerospace Sciences ATTN: J. Tien Cleveland, OH 44135
1	Battelle Memorial Institute ATTN: Tech Library 505 King avenue Columbus, OH 43201	3	Georgia Institute of Tech School of Aerospace Eng. ATTN: B. T. Zinn E. Price W. C. Strahle Atlanta, GA 30332
1	Brigham Young University Dept. of Chemical Engineering ATTN: M. Beckstead Provo, UT 84601	1	Institute of Gas Technology ATTN: D. Gidaspow 3424 S. State Street Chicago, IL 60616
1	California Institute of Tech 204 Karman Lab Main Stop 301-46 ATTN: F. E. C. Culick 1201 E. California Street Pasadena, CA 91125	1	Johns Hopkins University Applied Physics Laboratory Chemical Proplsion Information Agency ATTN: T. Christian Johns Hopkins Road Laurel, MD 20707
1	Director Jet Propulsion Laboratory 4800 Oak Grove Drive Pasadena, CA 91103	1	Massachusetts Institute of Tech Dept of Mechanical Engineering ATTN: T. Toong Cambridge, MA 02139
1	University of Illinois Dept. of Mech. Eng. ATTN: H. Krier 144 MEB, 1206 W. Green St. Urbana, IL 61801		

DISTRIBUTION LIST

No. Of Copies	Organization
1	Pennsylvania State University Applied Research Lab ATTN: G. M. Faeth P. O. Box 30 State College, PA 16801
1	Pennsylvania State University Dept. Of Mechanical Engineering ATTN: K. Kuo University Park, PA 16802
1	Purdue University School of Mechanical Engineering ATTN: J. R. Osborn TSPC Chaffee Hall West Lafayette, IN 47906
1	Rensselaer Polytechnic Inst. Department of Mathematics Troy, NY 12181
1	Rutgers University Dept. of Mechanical and Aerospace Engineering ATTN: S. Temkin University Heights Campus New Brunswick, NJ 08903
1	SRI International Propulsion Sciences Division ATTN: Tech Library 333 Ravenswood Avenue Menlo Park, CA 94025
1	Stevens Institute of Technology Davidson Laboratory ATTN: R. McAlevy, III Hoboken, NJ 07030
2	Los Alamos National Lab ATTN: Thomas Butler, MS B216 M. Division, B. Craig P. O. Box 1663 Los Alamos, NM 87545
1	University of Southern California Mechanical Engineering Dept. ATTN: OHE200, M. Gerstein Los Angelos, CA 90007
2	University of Utah Dept. of Chemical Engineering ATTN: A. Baer G. Flandro Salt Lake City, UT 84112
1	Washington State University Dept. of Mechanical Engineering ATTN: C. T. Crowe Pullman, WA 99163

Aberdeen Proving Ground

Dir, USAMSAA
ATTN: DRXSY-D
DRXSY-MP, H. Cohen

Cdr, USATECOM
ATTN: DRSTE-TO-F
STEAP-MT, S. Walton
G. Rice
D. Lacey
C. Herud

Dir, HEL
ATTN: J. Weisz

Dir, USACSL
Bldg. E3516, EA
ATTN: DRDAR-CLB-PA
DRDAR-CLN
DRDAR-CLJ-L

USER EVALUATION OF REPORT

Please take a few minutes to answer the questions below; tear out this sheet, fold as indicated, staple or tape closed, and place in the mail. Your comments will provide us with information for improving future reports.

1. BRL Report Number ____________________

2. Does this report satisfy a need? (Comment on purpose, related project, or other area of interest for which report will be used.)

____

____

____

3. How, specifically, is the report being used? (Information source, design data or procedure, management procedure, source of ideas, etc.) ____________________

____

____

4. Has the information in this report led to any quantitative savings as far as man-hours/contract dollars saved, operating costs avoided, efficiencies achieved, etc.? If so, please elaborate.

____

____

5. General Comments (Indicate what you think should be changed to make this report and future reports of this type more responsive to your needs, more usable, improve readability, etc.) ____________________

____

____

____

6. If you would like to be contacted by the personnel who prepared this report to raise specific questions or discuss the topic, please fill in the following information.

Name: ____________________

Telephone Number: ____________________

Organization Address: ____________________

____

____

FOLD HERE

Director
US Army Ballistic Research Laboratory
ATTN: DRDAR-BLA-S
Aberdeen Proving Ground, MD 21005

NO POSTAGE
NECESSARY
IF MAILED
IN THE
UNITED STATES

OFFICIAL BUSINESS
PENALTY FOR PRIVATE USE, $300

BUSINESS REPLY MAIL
FIRST CLASS PERMIT NO 12062 WASHINGTON, DC

POSTAGE WILL BE PAID BY DEPARTMENT OF THE ARMY

Director
US Army Ballistic Research Laboratory
ATTN: DRDAR-BLA-S
Aberdeen Proving Ground, MD 21005

FOLD HERE